

VILNIUS UNIVERSITY

CENTRE OF PHYSICAL SCIENCES AND TECHNOLOGY

Denis

SOKOL

Investigation of cation and anion  
substitution effects on the formation  
and properties of Mg-Al layered double  
hydroxides

**DOCTORAL DISSERTATION**

Natural sciences

Chemistry N 003

---

VILNIUS 2020

This dissertation was written during doctoral studies, between 2014 and 2018 at Vilnius University. The dissertation is defended on an external basis.

**Academic supervisor:**

**Prof. Habil. Dr. Aivaras Kareiva** (Vilnius University, Natural Sciences, Chemistry – N 003)

This doctoral dissertation will be defended in a public meeting of the Dissertation Defence Panel:

**Chairman – Prof. Habil. Dr. Albertas Malinauskas** (Centre for Physical Sciences and Technology, Natural Sciences, Chemistry – N 003).

**Members:**

**Prof. Dr. Jürg Hulliger** (University of Bern, Natural Sciences, Chemistry – N 003).

**Dr. Jurga Juodkazytė** (Centre for Physical Sciences and Technology, Natural Sciences, Chemistry – N 003).

**Prof. dr. Raimundas Šiaučiūnas** (Kaunas University of Technology, Technological Sciences, Chemical Engineering – T 005).

**Assoc. Prof. Dr. Aurimas Vyšniauskas** (Centre for Physical Sciences and Technology, Natural Sciences, Chemistry – N 003).

The dissertation shall be defended at a public meeting of the Dissertation Defence Panel at 2 pm on 3 July 2020 in Inorganic Chemistry auditorium 141 of the Institute of Chemistry, Faculty of Chemistry and Geoscience, Vilnius University.

Address: Naugarduko g. 24, LT-03225 Vilnius, Lithuania. Tel.: +370 5 2193108. Fax: +370 5 2330987.

The text of this dissertation can be accessed at the libraries of (name of the institutions granted the right to conduct doctoral studies in alphabetical order), as well as on the website of Vilnius University: [www.vu.lt/lt/naujienos/ivykiu-kalendorius](http://www.vu.lt/lt/naujienos/ivykiu-kalendorius)

VILNIAUS UNIVERSITETAS  
FIZINIŲ IR TECHNOLOGIJOS MOKSLŲ CENTRAS

Denis  
SOKOL

# Katijonų ir anijonų pakaitų įtakos Mg-Al sluoksniuotų dvigubų hidroksidų susidarymui ir savybėms tyrimas

**DAKTARO DISERTACIJA**

Gamtos mokslai,

Chemija N 003

---

VILNIUS 2020

Disertacija rengta 2014–2018 metais studijuojant doktorantūra Vilniaus universitete ir ginama eksternu.

**Mokslinis konsultantas:**

**prof. habil. dr. Aivaras Kareiva** (Vilniaus universitetas, gamtos mokslai, chemija – P 003).

Gynimo taryba:

Pirmininkas: **prof. habil. dr. Albertas Malinauskas** (Fizinių ir technologijos mokslų centras, gamtos mokslai, chemija – N 003).

Nariai:

**prof. dr. Jürg Hulliger** (Berno universitetas, gamtos mokslai, chemija – N 003).

**dr. Jurga Juodkazytė** (Fizinių ir technologijos mokslų centras, gamtos mokslai, chemija – N 003);

**prof. dr. Raimundas Šiaučiūnas** (Kauno technologijos universitetas, technologijos mokslai, chemijos inžinerija – T 005);

**doc. dr. Aurimas Vyšniauskas** (Fizinių ir technologijos mokslų centras, gamtos mokslai, chemija – N 003).

Disertacija bus ginama viešame Chemijos mokslo krypties gynimo tarybos posėdyje 2020 m. liepos 3 d. 14 val. Vilniaus universiteto Chemijos ir geomokslų fakulteto Chemijos instituto Neorganinės chemijos auditorijoje.

Adresas: Naugarduko g. 24, LT-03225 Vilnius, Lietuva. Tel.: 2193108.

Faksas: 2330987.

Disertaciją galima peržiūrėti Vilniaus universiteto, Fizinių ir technologijos mokslų centro bibliotekose ir VU interneto svetainėje adresu:

<https://www.vu.lt/naujienos/ivykiu-kalendorius>

## CONTENTS

LIST OF ABBREVIATIONS.....	7
INTRODUCTION.....	8
1. LITERATURE OVERVIEW.....	10
1.1. Basic Structural features of layered double hydroxides (LDHs).....	10
1.2. Brucite layer elements (Cations) in LDHs.....	13
1.3. Interlayer compounds (Anions) in LDHs .....	14
1.4. LDH Synthesis methods.....	14
1.5. Application of LDHs .....	15
2. EXPERIMENTAL.....	18
2.1. Materials.....	18
2.2. Synthesis methods.....	18
2.2.1. Synthesis of CoMg-Al LDH via co-precipitation method.....	19
2.2.2. Synthesis of $Mg_3Al_{1-x}Bi_x$ LDH via co-precipitation method.....	19
2.2.3. Synthesis of $Mg_3Al_{1-x}Bi_x$ LDH via aqueous sol-gel method.....	19
2.2.4. Synthesis of $Mg_2Al_1$ -hydroxide LDH via aqueous sol-gel method.....	20
2.2.5. Anion exchange in $Mg_2Al_1$ LDH from hydroxide to chloride.....	20
2.2.6. Anion exchange in $Mg_2Al_1$ LDH from chloride to phosphate.....	21
2.2.7. Synthesis of $Mg_2Al_1$ and $Mg_2Al_{0.9}Ce_{0.1}$ via aqueous sol-gel method.....	21
2.2.8. Anion exchange and formation of chloride- and phosphate- intercalated LDH.....	22
2.3. Characterization techniques.....	22
3. RESULTS AND DISCUSSION.....	24
3.1. Reconstruction effects on surface properties of Co/Mg/Al layered double hydroxide.....	24
3.1.1. Characterization of synthesized, decomposed and reconstructed LDHs.....	24
3.1.2. Characterization of LDHs specific surface area after thermal treatment.....	26
3.2. Bi-substituted $Mg_3Al-CO_3$ layered double hydroxides.....	28

3.2.1. Synthesis and characterization of $Mg_3Al_1$ and $Mg_3Al_{1-x}Bi_x$ LDHs produced via co-precipitation and aqueous sol-gel methods.....	28
3.2.2. Investigation of annealing temperature effect for sol-gel derived LDHs for successful reconstruction to layered structure.....	30
3.2.3. Investigation of LDHs reformation process in water back to layered structure from mixed-metal oxides (“memory effect”) .....	32
3.3. Dielectric properties of Bi-substituted LDHs synthesized by co-precipitation and sol-gel methods.....	34
3.3.1. Characterization of $Mg_3Al_{1-x}Bi_x$ LDH samples prepared via co-precipitation and aqueous sol-gel methods.....	34
3.3.2. Investigation the temperature dependence of dielectric permittivity of $Mg_3Al_{1-x}Bi_x$ LDH samples prepared by different methods.....	35
3.4. Sonication accelerated formation of Mg-Al-phosphate layered double hydroxide via sol-gel prepared mixed metal oxides.....	37
3.4.1 Temperature and high-power ultrasound effect on $Mg_2Al_{(MMO)}$ hydration .....	37
3.4.2 High-power ultrasound effect on LDH interlayer substitution, composition and morphology.....	39
3.5. Cast iron corrosion protection with chemically modified $Mg_2Al_1$ layered double hydroxides synthesized using a novel approach.....	44
3.5.1. Analysis and characterization of synthesized and substituted $Mg_2Al_1$ and $Mg_2Al_{0.9}Ce_{0.1}$ LDHs.....	45
3.5.2. Effect of LDHs to Electrochemical characterization and corrosion protection.....	49
4. CONCLUSIONS.....	55
5. LIST OF PUBLICATIONS AND CONFERENCES PARTICIPATION .....	57
5.1. Articles in journals .....	57
5.2. Attended conferences.....	57
6. ACKNOWLEDGEMENTS.....	59
7. REFERENCES.....	60
8. SUMMARY IN LITHUANIAN.....	66

## LIST OF ABBREVIATIONS

DTG - Derivative Thermogravimetry  
FTIR - Fourier Transform Infrared Spectroscopy  
LDH - Layered Double Hydroxide  
MMO - Mixed Metal Oxides  
TGA - Thermogravimetric Analysis  
SEM - Scanning Electron Microscopy  
XRD - X-ray diffraction  
STEM – Scanning transmission electron microscopy  
TEM - Transmission electron microscopy  
ICP-OES - inductive coupled plasma optical emission spectroscopy  
BET - Brunauer-Emmet-Teller method  
BJH - Barret-Joyner-Halenda method  
XRF - X-ray fluorescence technique  
HT - Hydrotalcite  
TAL - Terephthalate  
SCE - Saturated calomel reference electrode  
FWHM - The full width at half maximum  
EIS – Electrochemical impedance spectroscopy  
UV – Ultraviolet

## INTRODUCTION

Layered double hydroxides (LDH), also known as hydrotalcite-type compounds, belong to a family of anionic clays whose crystal structure is derived from brucite,  $\text{Mg}(\text{OH})_2$ . In the LDHs, the positively charged mixed metal cation hydroxide layer alternate with charge-compensating interlayer of anions  $\text{A}^{m-}$  coordinated by water molecules [1]. Although  $\text{M}^{\text{I}}\text{-M}^{\text{III}}$  LDHs are known [2, 3], the great majority of LDHs are of the  $\text{M}^{\text{II}}\text{-M}^{\text{III}}$  type. The general chemical formula of such LDHs can be represented as  $[\text{M}^{\text{II}}_{1-x}\text{M}^{\text{III}}_x(\text{OH})_2]^{x+}(\text{A}^{m-})_{x/m}\cdot z\text{H}_2\text{O}$  [1]. The  $\text{M}^{\text{II}}$  cation is usually magnesium or a 4<sup>th</sup>-period transition metal from iron to zinc, and  $\text{M}^{\text{III}}$  is, as a rule, Al, Ga, Fe, or Cr [3]. It has recently been demonstrated that some amount (an order of 10 mol%) of large trivalent cations, namely lanthanides [4-7] can substitute  $\text{M}^{\text{III}}$  in the LDH structure. The most used LDHs have the  $\text{M}^{\text{II}}/\text{M}^{\text{III}}$  cations ratio between 2 and 3, although it can be in the range from 1 to about 5 [1]. Different layer charge density created by the cations ratio and the natural flexibility of the crystal structure allows the formation of LDHs intercalated with a great variety of inorganic and organic anions [3, 8-15].

Layered double hydroxides have found various applications in many areas, such as catalysis, drug delivery, adsorption, separation, energy storage, hydrogen and oxygen evolution reactions, and corrosion protection [16-22]. Majority of the commercially produced LDHs are made by co-precipitation [23], by hydrothermal synthesis [24] or via the route that combines both these methods [25]. These synthetic techniques make possible a production of well-crystallized product with good reproducibility; however, they are rather time-consuming.

Therefore, the development of new synthetic approaches for LDHs is very important and timely task for materials scientists. The results presented in the current PhD thesis show considerable improvement not only in the synthesis procedure of LDHs, but in microstructural and physical properties of synthesized materials as well. Moreover, the search of novel LDHs chemical compositions by substituting magnesium and aluminium by other cations and introducing different anions offers a novelty and originality for the outgoing scientific investigations. Importantly, the obtained new LDHs showed specific properties, thus making its as suitable materials for different applications.

**The aim** of this PhD study was to investigate cation and anion substitution effects on the formation and properties of Mg-Al layered double hydroxides. To achieve this, the main tasks were formulated as follows:



1. To investigate the cobalt substitution effect in Co-Mg-Al LDHs obtained by co-precipitation method at low supersaturation on the surface properties of as synthesized and reconstructed in different reconstruction media LDHs.
2. To synthesize for the first time Bi<sup>3+</sup>-substituted Mg-Al LDHs using direct co-precipitation and novel indirect aqueous sol-gel methods and investigate an influence of different parameters on the formation of Bi-Mg-Al LDHs.
3. To examine dielectric properties of Bi-Mg-Al LDHs prepared by co-precipitation and aqueous sol-gel methods.
4. To investigate sonication effect on the reconstruction possibilities and anion substitution in Mg-Al LDHs synthesized via sol-gel method.
5. To investigate anticorrosion properties of chemically modified Mg-Al LDHs.

# 1. LITERATURE OVERVIEW

## 1.1. Basic Structural features of layered double hydroxides (LDHs)

Layered double hydroxides (LDHs), also known as hydrotalcite-type compounds, belong to a family of anionic clays whose crystal structure is derived from brucite,  $\text{Mg}(\text{OH})_2$ . The LDH phases differ in that some of the octahedral  $M^{2+}$  cations are replaced by  $M^{3+}$  cations, producing layers with a net positive charge. Positively charged layers of double metal hydroxides alternate with charge-compensating interlayer of anions coordinated by water molecules [1]. Although  $M^I$ - $M^{III}$  LDHs are known [2, 3], but the great majority of layered hydroxides are of the  $M^{II}$ - $M^{III}$  type. The general chemical formula of such LDHs can be represented as  $[M^{II}_{1-n}M^{III}_n(\text{OH})_2]^{n+}(A^{m-})_{n/m} \cdot z\text{H}_2\text{O}$ .

The metal cations in the hydroxide layers are coordinated by six oxygen atoms forming 2-D structures of the face-linked oxygen octahedra (Fig. 1). The octahedra are compressed in the direction perpendicular to the layer planes [1].

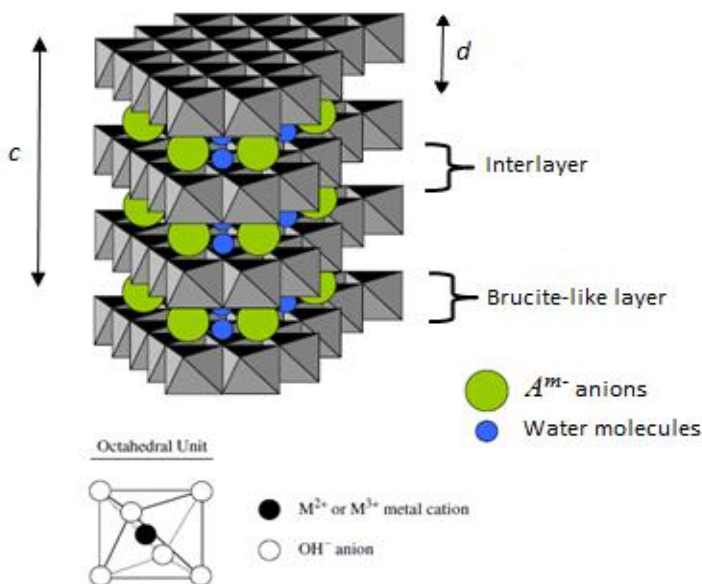


Fig. 1. A schematic representation of LDH structure of a 3R polytype where the lattice parameter  $c$  and the basal spacing  $d$  relate to each other as  $c = 3d$  [26-29].

LDHs are typically characterized by hexagonal symmetry with the *c*-axis perpendicular to the layers. The characteristic scale of the layer-interlayer structure (basal plane spacing, *d*) in LDH can be between about 0.75 nm to several nanometres depending on the composition and arrangement of species in the interlayer. The hydroxide layers can be stacked in different ways that results in different LDH polytypes (see Table 1).

Table 1. Hidrotalcite minerals and structures.

Name and chemical composition	Unit cell parameters		Symmetry
	<i>a</i> - Å	<i>c</i> - Å	
Hydrotalcite - $\text{Mg}_6\text{Al}_2(\text{OH})_{16}\text{CO}_3 \cdot 4\text{H}_2\text{O}$	3.054	22.81	3R
Manasseite - $\text{Mg}_6\text{Al}_2(\text{OH})_{16}\text{CO}_3 \cdot 4\text{H}_2\text{O}$	3.10	15.6	2H
Pyroaurite - $\text{Mg}_6\text{Fe}_2(\text{OH})_{16}\text{CO}_3 \cdot 4\text{H}_2\text{O}$	3.109	23.41	3R
Sjognerite - $\text{Mg}_6\text{Fe}_2(\text{OH})_{16}\text{CO}_3 \cdot 4.5\text{H}_2\text{O}$	3.113	15.61	2H
Stichtite - $\text{Mg}_6\text{Cr}_2(\text{OH})_{16}\text{CO}_3 \cdot 4\text{H}_2\text{O}$	3.10	23.4	3R
Barbertonite - $\text{Mg}_6\text{Cr}_2(\text{OH})_{16}(\text{OH})_2 \cdot 4\text{H}_2\text{O}$	3.10	15.6	2H
Takovite - $\text{Ni}_6\text{Al}_2(\text{OH})_{16}\text{CO}_3 \cdot 4\text{H}_2\text{O}$	3.025	22.59	3R
Reevesite - $\text{Ni}_6\text{Fe}_2(\text{OH})_{16}\text{CO}_3 \cdot 4\text{H}_2\text{O}$	3.08	22.77	3R
Desautelsite - $\text{Mg}_6\text{Mn}_2(\text{OH})_{16}\text{CO}_3 \cdot 4\text{H}_2\text{O}$	3.114	23.39	3R

The brucite-like sheets can stack one on the other with two different symmetries, rhombohedral or hexagonal. If we call ABC the three-fold axis of the OH groups in the brucite-like sheet, the stack may have the sequence BC-CA-AB-BC, thus having three sheets in the unit cell, or BC-CB-BC with two sheets in the unit cell with hexagonal symmetry. The XRD patterns of synthetic LDHs are presented in Fig. 2. The specimens of rhombohedral symmetry have mainly been found in nature; the hexagonal polytype may be the high temperature form of the rhombohedral one. In fact, hexagonal

symmetry has been discovered in the interior of some mineral crystals, while the rhombohedral type is maintained in the external part; the transformation occurs during the cooling of the mineral, but due to the energy barrier the hexagonal form can no longer transform at low temperature [1, 28].

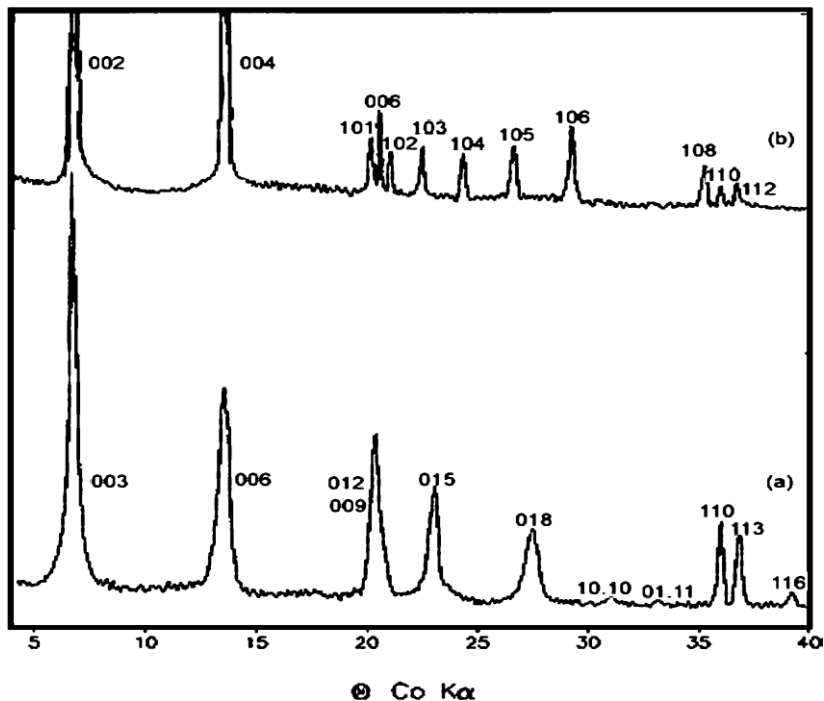


Fig. 2. XRD patterns of synthetic hydrotalcite  $[\text{Mg}_6\text{Al}_2(\text{OH})_{16}](\text{CO}_3)\cdot 4\text{H}_2\text{O}$  which has a **3R** polytype (a) and the mineral manasseite which has the same formula as hydrotalcite but a **2H** polytype (b) [26-29].

Therefore, the  $c$ -parameter is multiply of  $d$  with a factor of either 3 or 2 depending on the polytype (Fig. 2, Table 1). The basal spacing value depends on size, charge and orientation of the intercalated anions as well as the relative amount of crystal water. Parameter  $a$  is a function of both the  $M^{\text{II}}$  and  $M^{\text{III}}$  cations size and ratio, and is typically within 0.30-0.31 nm. The lattice parameters  $a$  and  $c$  can be independently calculated from the angle positions of the (110) diffraction reflection and the (00l) reflections family, respectively (Fig. 3).

## 1.2. Brucite layer elements (Cations) in LDHs

Numbers of synthetic pairs of  $M^{\text{II}}-M^{\text{III}}$  cations were experimentally used to estimate the ranges of the relative sizes of the cations that can form an LDH structure. In a majority of the known  $M^{\text{II}}-M^{\text{III}}$  LDH, but there is also  $M^{\text{I}}-M^{\text{III}}$  [31, 32].  $M^{\text{II}}$  is cation of magnesium or a 4<sup>th</sup>-period transition metal from iron to zinc ( $\text{Mn}^{2+}$ ,  $\text{Fe}^{2+}$ ,  $\text{Co}^{2+}$ ,  $\text{Ni}^{2+}$ ,  $\text{Cu}^{2+}$ ,  $\text{Zn}^{2+}$ ), and  $M^{\text{III}}$  is, as a rule,  $\text{Al}^{3+}$ ,  $\text{Ga}^{3+}$ ,  $\text{Fe}^{3+}$  or  $\text{Cr}^{3+}$  [3]. In such combinations, the divalent metal cation from 0.65 Å to 0.80 Å is slightly bigger than the trivalent one, from 0.50 Å to 0.69 Å. At the same time, the LDH compounds containing the relatively large  $M^{\text{II}}$  cations, namely  $\text{Ca}^{2+}$  (1.00 Å) [32, 33],  $\text{Cd}^{2+}$  (0.95 Å) [34],  $\text{Ba}^{2+}$  (1.35 Å) [35] were successfully prepared and thoroughly characterized. It has recently been demonstrated that some amount (an order of 10 %) of large trivalent cations with ionic radii from 0.9 Å to 1.11 Å, mainly group of lanthanides (Ln) or rare earth metals  $\text{Ce}^{3+}$  [4, 5, 36],  $\text{Nd}^{3+}$  [4, 6, 37],  $\text{Sm}^{3+}$  [6, 37],  $\text{Eu}^{3+}$  [4, 6, 37],  $\text{Tb}^{3+}$  [4, 37],  $\text{Er}^{3+}$  [4, 37],  $\text{Yb}^{3+}$  [4, 37],  $\text{Dy}^{3+}$  [37],  $\text{Ho}^{3+}$  [37],  $\text{Y}^{3+}$  [37] and  $\text{Gd}^{3+}$  [37] can substitute  $M^{\text{III}}$  in the LDH structure.

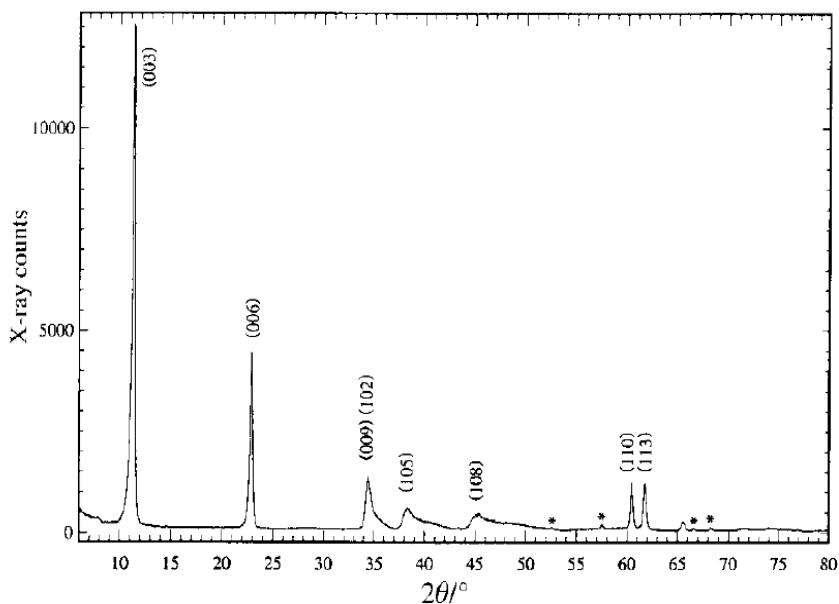


Fig.3. XRD pattern of the HT-Mg-Al- $\text{CO}_3$  at room temperature. The asterisks indicate reflections due to the impurity  $\text{Al}_2\text{O}_3$  [30].

### 1.3. Interlayer compounds (Anions) in LDHs

The most used LDHs have the  $M^{II}/M^{III}$  cations ratio between 2 and 3, although it can be in the range from 1 to about 5 [1, 28]. Different layer charge density conditioned by the cations ratio and the natural flexibility of the crystal structure allows formation of LDHs intercalated with a great variety of inorganic anions  $F^-$ ,  $Cl^-$ ,  $Br^-$ ,  $I^-$ ,  $ClO_4^-$ ,  $NO_3^-$ ,  $ClO_3^-$ ,  $IO_3^-$ ,  $OH^-$ ,  $CO_3^{2-}$ ,  $SO_4^{2-}$ ,  $S_2O_3^{2-}$ ,  $WO_4^{2-}$ ,  $CrO_4^{2-}$ ,  $[Fe(CN)_6]^{3-}$ ,  $[Fe(CN)_6]^{4-}$ ,  $[SiO(OH)_3]^-$ ; [3, 28], among them the most occurred are  $Cl^-$  [8, 9],  $OH^-$  [10],  $CO_3^{2-}$  [11],  $PO_4^{3-}$  [12-14], and organic anions of organic acids adipic, oxalic, succinic, malonic, sebacic, 1,12- dodecanedicarboxylic acid, acyl and arylsulphonates, chlorocinnamic acid [3, 15, 28].

There is practically no limitation to the nature of the anions which can compensate for the positive charge of the brucite-like sheet; the only problem can be related to the preparation of pure or well crystallized materials. For example, when preparing LDHs containing anions different from carbonate, it is very difficult to avoid contamination from the  $CO_2$  present in the aqueous solution.

The number, the size, the orientation, and the strength of the bonds between the anions and the hydroxyl groups of the brucite-like layers determine the thickness of the interlayer –  $c$ , which can be calculated from XRD pattern [1, 28]. Also when LDHs are intercalated with single-atom anions or with some other simple anions that are arranged parallel to the hydroxide layers, the crystal symmetry is known [8]. However, in the cases of large polyatomic anions [3, 9, 28], the real symmetry of the crystal lattice can be lower than rhombohedral or still rhombohedral but with a higher value of  $a$ -parameter. This results in appearance of additional peaks in the XRD pattern that complicates identification of LDH phase. Despite all difficulties of making Anion substituted LDHs, they have a great interest and wide range of application [38].

### 1.4. LDH Synthesis methods

LDHs have been synthesized by direct methods, such as co-precipitation, sol-gel synthesis, hydrothermal growth, combustion synthesis, electrochemical synthesis and synthesis using microwave irradiation [39-41]. The most common method applied for the preparation of LDHs is the co-precipitation [42-45]. The precipitating agents NaOH or  $NaHCO_3$  are added

to the prepared solution of starting materials. The LDHs precipitates and form homogenous mixtures if solubility products of the metal hydroxides are very similar. Low supersaturation conditions usually give rise to more crystalline precipitates. The direct sol-gel method for the preparation of LDHs has some limitations, since amorphous materials could be obtained. Another feature that makes these sol-gel materials distinguishable from those prepared by other synthetic methods is their high specific surface area [39]. However, if metal alkoxides in the sol-gel processing are used as starting materials, the synthesis conditions should be more strictly controlled than in the co-precipitation method [39, 40]. Besides, the synthesis processing in that case is rather expensive. Improved crystalline structures can be obtained by hydrothermal treatment in the presence of water vapour at temperatures not exceeding the decomposition temperature of the LDHs. While heating the reactants in a pressurized aqueous media improves the crystallinity of the resulting LDHs, however, the hydrothermal synthesis may require additional effort and time. This method can also result in a decrease of surface area and growth of hydrocalcite crystals [40]. The preparation of Mg/Al hydrocalcite-like compounds by combustion, electrochemical and microwave irradiation syntheses has also been reported. The drawbacks of these proposed techniques are the materials have a poor crystallinity, time-consuming and rather expensive processes. Besides, high number of surface-defective sites could be induced.

Recently, a novel, simple, cost effective and environmentally friendly indirect sol-gel synthesis route was developed for the preparation of Mg-Al LDHs [5-7, 41, 46]. The main advantages of this sol-gel method for the preparation of LDHs are high homogeneity, phase purity and high reproducibility of the final products. These features are very important to study substitutions effects in the LDHs. The conversion of the mixed metal oxides into LDHs has been variously referred to as regeneration, reconstruction, restoration, rehydration or the “calcination-rehydration process”, “structural memory effect” or simply “memory effect” [38]. This method is usually employed when large guests are intercalated.

### 1.5. Application of LDHs

LDHs are widely used as adsorbents for liquid ions and gas molecules, and can be applied for the removal of anionic toxins during water purification and also toxic metals ions [38, 46-50]. They also find use as catalysts for oxidation,

reduction and other catalytic reactions [38, 46, 51-54]. The LDHs intercalated with bioactive molecules could be used in medicine for biosensing, in cancer therapy and as drug and gens delivery systems [55-61]. LDHs show good promise for application in sensor devices and in membrane reactors for the production of hydrogen. The schematic diagram of possible applications of LDHs is shown in Fig. 4.

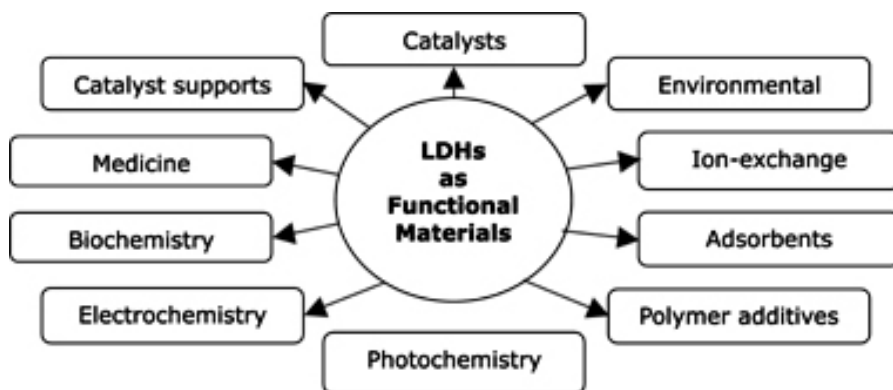


Fig. 4. The schematic diagram of possible applications of LDHs.

The LDHs layers were demonstrated to offer an anticorrosion protection [62-66]. These inhibitors create a passive insoluble oxide layer that stops the oxygen diffusion from the aggressive environment to the surface. In recent years, LDHs were widely investigated as promising luminescence materials due to the novel properties to form stable compounds with lanthanides in the interlayer space of LDH [5, 6, 67-75]. For example, the luminescent properties of the sol-gel derived  $Mg_3Al_{1-x}Nd_x$  LDHs were investigated in [75]. Unfortunately, these neodymium-substituted layered double hydroxides as prepared did not demonstrate any luminescence, even though XRD patterns and SEM morphology have been showed the monophasic  $Mg_3Al_{1-x}Nd_x$  LDH formation. The attempt to generate the luminescence by intercalating terephthalate (TAL) in these LDH samples was made. The emission spectra of  $Mg_3Al_{1-x}Nd_x$  1-10 mol%- TAL LDH samples in the near-red region given by excitation at 580 nm are shown in Fig. 5.



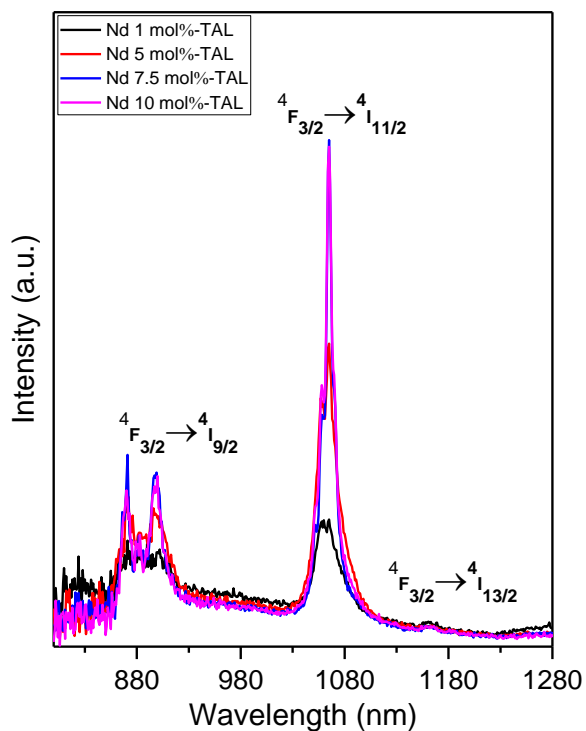


Fig. 5. Emission spectra of  $\text{Mg}_3\text{Al}_{1-x}\text{Nd}_x$  1-10 mol%-TAL LDHs (Ex=580 nm).

As seen, the emission spectra contain several bands located at 900 and 1065 nm. The interlayer TAL anions act as an energy antenna to the central  $\text{Nd}^{3+}$  ions enhancing the luminescence [75].

## 2. EXPERIMENTAL

### 2.1 Materials

The following materials were used for synthesis and anion modification of LDHs: aluminium nitrate nonahydrate ( $\text{Al}(\text{NO}_3)_3 \cdot 9\text{H}_2\text{O}$ ,  $\geq 98.5\%$ , Sigma-Aldrich), magnesium nitrate hexahydrate ( $\text{Mg}(\text{NO}_3)_2 \cdot 6\text{H}_2\text{O}$ , 99%, Sigma-Aldrich), cobalt nitrate hexahydrate ( $\text{Co}(\text{NO}_3)_2 \cdot 6\text{H}_2\text{O}$ , 98%, Sigma-Aldrich) bismuth nitrate pentahydrate ( $\text{Bi}(\text{NO}_3)_3 \cdot 5\text{H}_2\text{O}$ , 98%, Fluka), cerium nitrate hexahydrate ( $\text{Ce}(\text{NO}_3)_3 \cdot 6\text{H}_2\text{O}$ , 99.99%, Sigma-Aldrich), sodium chloride ( $\text{NaCl}$ , 99.9%, Sigma-Aldrich), ethylene glycol ( $\text{C}_2\text{H}_6\text{O}_2$ , 99%, Sigma-Aldrich), hydrochloric acid ( $\text{HCl}$ , 36%, Chempur), sodium phosphate dibasic dihydrate ( $\text{NaH}_2\text{PO}_4 \cdot 2\text{H}_2\text{O}$ ,  $>98\%$ , Carl Roth), sodium dihydrogen phosphate ( $\text{NaH}_2\text{PO}_4 \cdot 2\text{H}_2\text{O}$ ,  $>98\%$ , Carl Roth), acetic acid ( $\text{CH}_3\text{COOH}$ , 99%, REACHEM), nitric acid ( $\text{HNO}_3$ , 66%, REACHEM), sodium hydrogen carbonate ( $\text{NaHCO}_3$ , 99.7%, Sigma-Aldrich), sodium hydroxide ( $\text{NaOH}$ , 98%, Sigma-Aldrich). The cast iron (GG20) samples were provided by SEW-EURODRIVE Portugal LDA.

### 2.2. Synthesis methods

#### 2.2.1. Synthesis of CoMg-Al LDH via co-precipitation method

CoMg-Al LDHs were prepared by the coprecipitation under low supersaturation from a solution of the appropriate metal nitrates with a molar ratio of  $(\text{Co}+\text{Mg}):\text{Al} = 3:1$  and a solution of  $\text{NaHCO}_3:\text{NaOH}$  with a molar ratio of 1:2. During the preparation, 15% of the  $1 \text{ mol L}^{-1} \text{ Mg}(\text{NO}_3)_2$  solution was replaced by a  $1 \text{ mol L}^{-1} \text{ Co}(\text{NO}_3)_2$  solution. The solution of metal nitrates was added very slowly to the solution of  $\text{NaHCO}_3+\text{NaOH}$  ( $\text{pH} \approx 12$ ) under vigorous stirring. After mixing the obtained gel was aged at 353 K for 6 h. The slurry was filtered and washed with distilled water and dried in open air. The resulting powder was marked as Co/Mg/Al. The mixed-metal oxide obtained by subsequent heating at 923 K for 3 h was labelled as  $\text{Co/Mg/Al}_{\text{cal}}$ . The reconstruction of LDHs from  $\text{Co/Mg/Al}_{\text{cal}}$  was performed in water at  $\text{pH} \approx 6$  (2 g of mixed oxide in 40 mL of water) and in magnesium nitrate solution at  $\text{pH} \approx 3.7$  (2 g of mixed oxide in 40 mL of  $1 \text{ mol L}^{-1} \text{ Mg}(\text{NO}_3)_2$ ) at 293 K and 353 K for 6 h. The samples reconstructed in water were labelled as

Co/Mg/Al<sub>W293</sub>, Co/Mg/Al<sub>W353</sub> and the specimens reconstructed in nitrate media were named as Co/Mg/Al<sub>N293</sub>, Co/Mg/Al<sub>N353</sub>. After the reconstructed processes, the samples were washed with water and dried in air.

### 2.2.2. Synthesis of Mg<sub>3</sub>Al<sub>1-x</sub>Bi<sub>x</sub> LDH via co-precipitation method

Mg<sub>3</sub>Al<sub>1</sub> LDH was prepared by the co-precipitation under low super saturation out of a solution of the appropriate metal nitrates Al(NO<sub>3</sub>)<sub>3</sub>·9H<sub>2</sub>O and Mg(NO<sub>3</sub>)<sub>2</sub>·6H<sub>2</sub>O with a molar ratio of Mg:Al = 3:1 and a solution of NaHCO<sub>3</sub>:NaOH with a molar ratio of 1:2. The solution of metal nitrates was slowly poured into the solution of NaHCO<sub>3</sub>+NaOH (pH ≈12) under vigorous stirring. After mixing, the obtained slurry was aged at a temperature of 80 °C for 6 h. The slurry was filtered and washed with distilled water and dried in an oven at a temperature of 60 °C. The resulting powders were labelled as Mg<sub>3</sub>Al<sub>1(co-pr)</sub>. The mixed-metal oxide obtained by subsequent heating at a temperature of 650 °C for 3 h was labelled as Mg<sub>3</sub>Al<sub>1(co-pr/cal)</sub>. The hydration was carried out in water at a temperature of 80 °C for 6 h at pH ≈8.5. The LDH sample restored in water was labelled as Mg<sub>3</sub>Al<sub>1(co-pr/W80)</sub>. Synthesis of Mg<sub>3</sub>Al<sub>1-x</sub>Bi<sub>x</sub> compounds was carried out in the same way as Mg<sub>3</sub>Al<sub>1</sub> LDH except Bi(NO<sub>3</sub>)<sub>3</sub>·5H<sub>2</sub>O was dissolved in 1M HNO<sub>3</sub>, since Bi(NO<sub>3</sub>)<sub>3</sub>·5H<sub>2</sub>O is insoluble in water. Mg<sub>3</sub>Al<sub>1-x</sub>Bi<sub>x(co-pr)</sub> compounds were prepared using cation molar ratio from x = 0.1 to x = 0.5. The mixed-metal oxides obtained by subsequent heating of Mg<sub>3</sub>Al<sub>1-x</sub>Bi<sub>x(co-pr)</sub> at 650 °C for 3 h were labelled as Mg<sub>3</sub>Al<sub>1-x</sub>Bi<sub>x(co-pr/cal)</sub>, (x = 0.1 to x = 0.5). The hydration was carried out also in water at 80 °C for 6 h at pH ≈8.5. The samples restored in water were labelled as Mg<sub>3</sub>Al<sub>1-x</sub>Bi<sub>x(co-pr/W80)</sub>. After the restoration processes, the samples were washed with water and dried in air.

### 2.2.3. Synthesis of Mg<sub>3</sub>Al<sub>1-x</sub>Bi<sub>x</sub> LDH via aqueous sol-gel method

Mg<sub>3</sub>Al<sub>1</sub> LDH was prepared by mixing the solutions of the appropriate metal nitrates with a molar ratio of Mg:Al = 3:1. The nitrates were dissolved in 50 ml of distilled water with addition of 50 ml of 0.2M acetic acid. Then, the solution has been stirred for 1 h at 80 °C. Next, 2 ml of ethylene glycol was added under continuous stirring for 4 h at the same temperature. After slow evaporation of solvent, the obtained gel was dried at 120-140 °C for 10-14 h (obtained compound was labelled as Mg<sub>3</sub>Al<sub>1(sg)</sub>). The mixed-metal oxide

obtained by subsequent heating of the precursor gel at 650 °C for 3 h was labelled as  $Mg_3Al_{1(sg/cal)}$ . The hydration of  $Mg_3Al_{1(sg/cal)}$  was carried out in water at 80 °C for 6 h at pH  $\approx$ 8.5. The sample restored in water was labelled as  $Mg_3Al_{1(sg/W80)}$ . Synthesis of  $Mg_3Al_{1-x}Bi_x$  compounds was carried out in the same way as  $Mg_3Al_1$  except  $Bi(NO_3)_3 \cdot 5H_2O$  was dissolved in 1M  $HNO_3$ .  $Mg_3Al_{1-x}Bi_x(sg)$  compounds were synthesized using cation molar ratio from  $x = 0.1$  to  $x = 0.5$ . The mixed-metal oxides were obtained by subsequent heating of  $Mg_3Al_{1-x}Bi_x(sg)$  at 650 °C for 3 h and were labelled as  $Mg_3Al_{1-x}Bi_x(sg/cal)$ . The hydration was carried out in water at 80 °C for 6 h at pH  $\approx$ 8.5. The samples restored in water were labelled as  $Mg_3Al_{1-x}Bi_x(sg/W80)$ . After the restoration processes, the samples were washed with water and dried in air.

#### 2.2.4. Synthesis of $Mg_2Al_1$ -hydroxide LDH via aqueous sol-gel method

$Mg_2Al$  precursor was prepared by mixing the solutions of the appropriate metal nitrates with a molar ratio of  $Mg/Al = 2:1$ . The nitrates were dissolved in 50 ml of distilled water with addition of 50 ml of a 0.2 M nitric acid. The solution was stirred for 1 h at 80°C. Then 2 ml of ethylene glycol were added under continuous stirring for 4 h at the same temperature. After slow evaporation of solvent, the obtained gel was dried at 120-140°C for 10-14 h. The  $Mg_2Al$  MMO was obtained by calcination of the precursor gel at 650°C for 3 h (hereafter labelled as  $Mg_2Al_{(MMO)}$ ). This calcination temperature was shown to be optimal for production of Mg-Al MMO that demonstrate the most complete transformation into a respective LDH phase upon hydration [5]. Hydration of the  $Mg_2Al_{(MMO)}$  powder in water was carried out under three different conditions, namely i) at room temperature with a vigorous mechanical stirring for defined time X of 15, 30 min, 1, 2, 4, 8, and 24 h; ii) at 80°C with stirring for 15, 30 min, 1, 2, 4, 8, and 24 h; and iii) at high-power sonication applied for 2, 4, 8, 15, and 30 min. The final powder samples were obtained by vacuum filtration and drying at 60°C for 30 min ( $Mg_2Al-OH_{(25^\circ C/X)}$ ,  $Mg_2Al-OH_{(80^\circ C/X)}$  and  $Mg_2Al-OH_{(Sonic/X)}$ , respectively).

#### 2.2.5. Anion exchange in $Mg_2Al_1$ LDH from hydroxide to chloride

Anion exchange was performed in 250 ml of a 1 M NaCl solution with addition of 0.3 ml of hydrochloric acid (36%). 1 g of  $Mg_2Al-OH_{(80^\circ C/24h)}$  was used. The reaction was carried out under two different conditions: i) at 25°C

with stirring for 15, 30 min, 1, 2, 4, 8, and 24 h; and ii) at high-power sonication applied for 2, 4, 8, 15, and 30 min. The final products ( $Mg_2Al-Cl_{(25^\circ C/X)}$  and  $Mg_2Al-Cl_{(Sonic/X)}$ , respectively) were obtained by vacuum filtration without any additional washing followed by drying for 30 min at  $60^\circ C$ .

#### 2.2.6. Anion exchange in $Mg_2Al_1$ LDH from chloride to phosphate

1 g of  $Mg_2Al-Cl_{(25^\circ C/24h)}$  was immersed into a 0.1 M  $Na_2HPO_4$  solution with addition of small amount of  $NaH_2PO_4$  to adjust the pH value to 7.5. This reaction was carried out either at  $25^\circ C$  with vigorous mechanical stirring or at high-power sonication applied for the same respective time intervals as those used the hydroxide-to-chloride exchange (see part Anion exchange in  $Mg_2Al$  LDH from hydroxide to chloride). The samples labelled as  $Mg_2Al-H_xPO_4_{(25^\circ C/X)}$  and  $Mg_2Al-H_xPO_4_{(Sonic/X)}$ , respectively, were obtained by vacuum filtration without any additional washing followed by drying for 30 min at  $60^\circ C$ .

#### 2.2.7. Synthesis of $Mg_2Al_1$ and $Mg_2Al_{0.9}Ce_{0.1}$ via aqueous sol-gel method

Appropriate metal nitrates were dissolved in 50 ml of distilled water with addition of 50 ml of 0.2 M nitric acid. To prepare Mg-Al (Mg-Al-Ce) metal oxides, the solutions were mixed with a molar ratio of Mg:Al = 2:1 (Mg:Al:Ce = 2:0.9:0.1). The obtained mixtures were stirred for 1 h at  $80^\circ C$ . Then 2 ml of ethylene glycol was added with continuous stirring for 4 h at the same temperature. After slow evaporation of solvent, the obtained gel was dried at  $130^\circ C$  for 12 h. Mixed metal oxides (MMO) of the  $Mg(2)Al$  and  $Mg(2)Al-10\%Ce$  cation compositions were produced by calcination of the dried gel powders for 3 h at  $650^\circ C$ . The layered double hydroxides were formed as a result of hydration of the MMO powders in deionized water at room temperature. To accelerate the process, high-power sonication was applied for 30 min. This stage of LDH formation (synthesis) as well the sonication-assisted anion exchange reactions were performed using a VCX 1500 Sonics processor (max output power 1.5 kW at 20 kHz) equipped with a high-volume continuous flow cell. The final powder LDH samples were obtained by vacuum filtration followed by drying at  $60^\circ C$  for 24 hours.

## 2.2.8. Anion exchange and formation of chloride- and phosphate-intercalated LDH

For a  $\text{OH}^- \rightarrow \text{Cl}^-$  anion-exchange, 1 g of  $\text{Mg}(2)\text{Al-OH}$  was added to 250 ml of 1 M  $\text{NaCl}$  solution at room temperature. The mixture was sonicated for 4 min. The obtained slurry was put in vacuum filtration without any additional washing and dried for 24 hours at  $60^\circ\text{C}$ . Chloride-to-phosphate anion exchange was carried out in a 0.1 M  $\text{Na}_2\text{HPO}_4$  solution at room temperature. 1 g of the  $\text{Mg}(2)\text{Al-Cl}$  powder was immersed in the solution followed by addition of  $\text{NaH}_2\text{PO}_4$  to adjust the pH value to 7.5. At such conditions, the intercalated anion is dihydrogen phosphate,  $\text{H}_2\text{PO}_4^-$  [14]. The reaction was sonication-assisted and took 8 min. The obtained slurry was filtered and dried at the same conditions as mentioned above. Similar process was used for the hydroxide-to-chloride and chloride-to-phosphate exchange reactions in  $\text{Mg}(2)\text{Al-10\%Ce}$  LDHs.

## 2.3. Characterization techniques

The X-ray powder diffraction (XRD) patterns of the samples were recorded with a conventional Bragg-Brentano geometry ( $\theta - 2\theta$  scans) on Rigaku MiniFlexII diffractometer, or DRON-6 automated diffractometer, or PANalytical X'Pert Powder diffractometer using  $\text{Cu K}\alpha$  radiation ( $\lambda = 1.541838 \text{ \AA}$ ). The cell parameters  $a$  and  $c$  of the rhombohedral structure were determined from the positions of the (110) and (003), (006) diffraction lines, respectively. The lattice parameter  $a = 2d(110)$  corresponds to an average cation-cation distance calculated from the 110 reflection, while the  $c$  parameter corresponds to three times the thickness of  $d(003)$  parameter. In this case  $c$  was calculated from two diffraction lines using equation  $c = 3/2 [d(003) + 2d(006)]$ . Morphology of synthesized compounds were investigated by scanning electron microscopy (SEM) using scanning electron microscopes Hitachi SU-70 or Hitachi HD-2700. Thermogravimetric (TG) analysis was carried out using PerkinElmer STA6000 apparatus or with a Netzsch STA 409 PC Luxx instrument. Fourier transform infrared (FTIR) spectra of the samples were recorded with a Perkin Elmer spectrum BX FTIR spectrometer. The specific surface area was evaluated by the Brunauer-Emmet-Teller method (BET) and the pore-size distribution by the Barret-Joyner-Halenda (BJH) procedure. The measurements were carried out on a Quantachrome Autosorb-1MP instrument using the program Autosorb. Metal loadings of the LDHs

were analyzed by X-ray fluorescence technique (XRF) on a Spectro Analytical Instrument GmbH&Co.KG spectrometer with a Pd window X-ray tube. Dielectric measurements were performed using HP4284A precision LCR meter in 1.2 kHz–1 MHz frequency range during cooling with 1.5–2 K/min rate. The samples were in a form of tablet, 1.6 mm thick with silver paste used to produce contact area of 49.3 mm<sup>2</sup>. Sonication-assisted experiments were performed using a VCX 1500 Sonics processor (max output power 1.5 kW at 20 kHz) equipped with a continuous flow cell. For the electrochemical measurements, a three-electrode cell with a large platinum auxiliary electrode, a saturated calomel reference electrode (SCE) and a working electrode with an exposed area of 1 cm<sup>2</sup> bare cast iron was used. The electrochemical impedance measurements were performed using the Autolab PGSTAT30 over a frequency range of 100 kHz–10 mHz with seven points per decade.

### 3. RESULTS AND DISCUSSION

#### 3.1. Reconstruction effects on surface properties of Co/Mg/Al layered double hydroxide

In this part of PhD thesis, the synthesis by co-precipitation method at low supersaturation was chosen as a direct route to prepare Co/Mg/Al LDH materials. The surface area and porosity as important characteristics of these materials were investigated in detail.

##### 3.1.1. Characterization of synthesized, decomposed and reconstructed LDHs.

The XRD patterns of synthesized, decomposed and reconstituted LDHs are shown in Fig. 6.

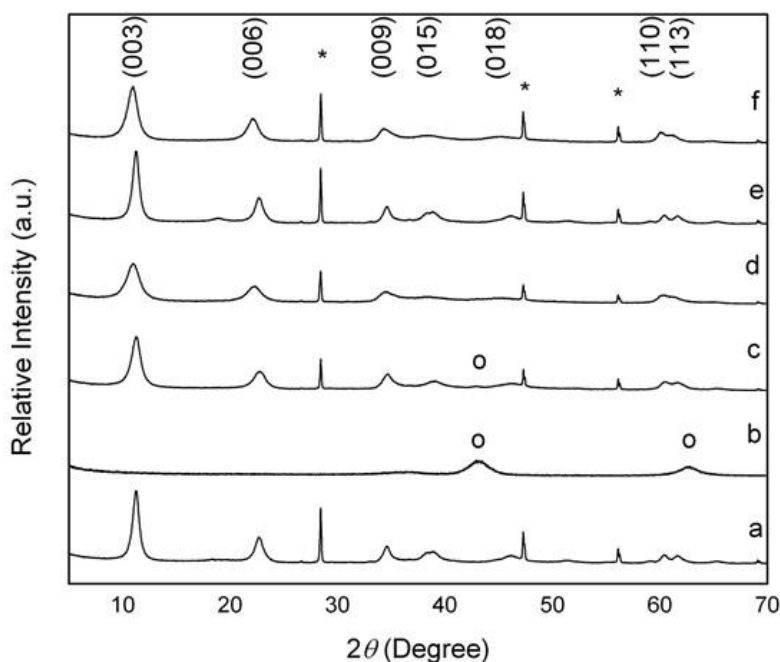


Fig. 6. XRD patterns of synthesized, decomposed and reconstructed LDHs: a - Co/Mg/Al; b - Co/Mg/Al<sub>cal</sub>; c - Co/Mg/Al<sub>W293</sub>; d - Co/Mg/Al<sub>N293</sub>; e - Co/Mg/Al<sub>W353</sub>; f - Co/Mg/Al<sub>N353</sub>. Additional phases are marked: o - MgO and \* - Si used as a reference.



The characteristic hydroxide type structure of as-synthesized sample Co/Mg/Al was confirmed by the XRD analysis data (Fig. 6a) [76]. The calculated cell parameter  $c = 23.6 \text{ \AA}$  (Table 2) for the synthesized LDH sample is slightly higher compared to the published value of  $23.4 \text{ \AA}$  for carbonate-containing Mg/Al LDHs [77]. After thermal decomposition only two broad reflections located at around  $2\theta = 43\text{-}44^\circ$  and  $62\text{-}63^\circ$  are seen in the XRD pattern. The XRD analysis of heat-treated sample revealed the formation of poorly crystalline magnesium oxide. The XRD patterns of LDH samples obtained after the hydration process at 293 and 353 K are given in Fig. 6c and Fig. 6e, respectively. At room temperature, an incomplete regeneration was observed in water since a weak MgO reflections were present in the XRD pattern. Interestingly, this oxide phase disappeared when the reconstruction process was carried out at higher temperature (353 K), suggesting the significance of the medium temperature on the reformation of LDHs.

Table 2. Crystallographic data and crystallite size of synthesized and reconstructed LDHs.

Sample	$d_{003}$ ( $\text{\AA}$ )	$d_{006}$ ( $\text{\AA}$ )	$d_{110}$ ( $\text{\AA}$ )	Cell parameters ( $\text{\AA}$ )		Crystallite size ( $\text{\AA}$ )
				$c$	$a$	
				Co/Mg/Al	7.93	
Co/Mg/Al <sub>W293</sub>	7.88	3.90	1.53	23.52	3.06	91
Co/Mg/Al <sub>N293</sub>	8.08	3.99	1.53	24.10	3.07	61
Co/Mg/Al <sub>W353</sub>	7.89	3.91	1.53	23.57	3.06	131
Co/Mg/Al <sub>N353</sub>	8.12	4.01	1.54	24.22	3.08	80

The basal spacing represents the thickness of a single layer and is normally related to the size of charge balancing interlayer anions. For the samples reconstructed in the magnesium nitrate solution, the  $d_{003}$  values are higher than  $8 \text{ \AA}$ .

### 3.1.2. Characterization of LDHs specific surface area after thermal treatment.

The influence of reconstruction process on the specific surface area and pore size of mixed metal oxides obtained from reconstructed LDHs by heating in air at 923 K were investigated. The N<sub>2</sub> adsorption-desorption isotherms of heat-treated cobalt containing LDHs exhibited type IV isotherms with an H1 hysteresis which are characteristic for the mesoporous materials. The t-plot analysis by de Boer method showed the absence of micropores. An increase at high relative pressure indicated interparticle porosity, which seems to show that the formed mixed oxides consist mainly of non-porous nanoparticles within the nanometer range (Fig. 7). The pore size distribution for all samples showed one main maximum between 50–130 Å except for Co/Mg/Al<sub>N293</sub> which displayed two maxima at 19 and 100 Å. The mixed oxide samples containing cobalt showed a decrease in total pore volume and an increase of average pore diameter when compared to Co/Mg/Al<sub>cal</sub> material. The chosen process to form mixed oxides (synthesis of LDH – calcination – reconstruction to LDH – second calcination) showed minor effects on pore dimensions.

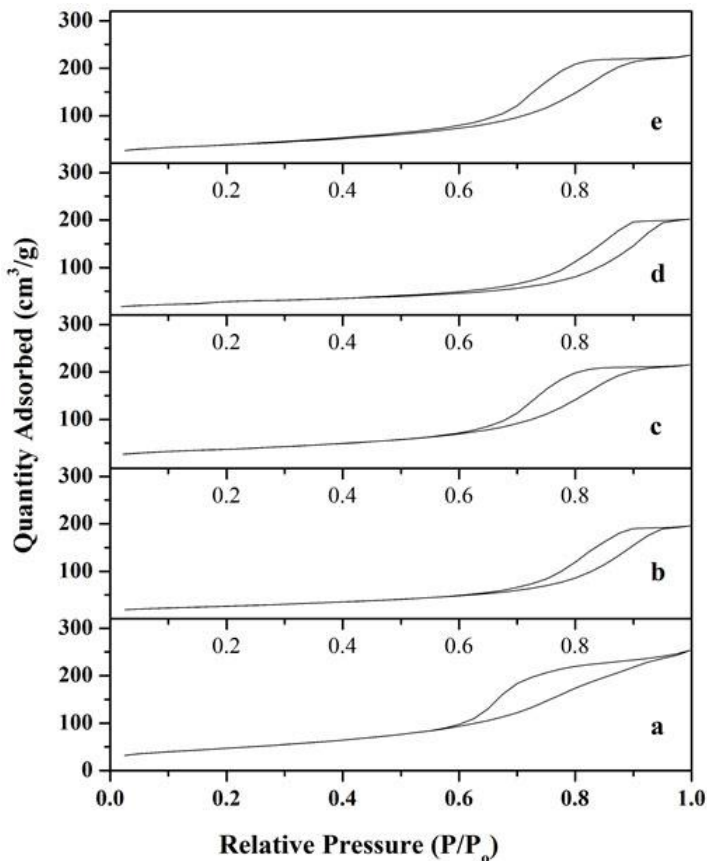


Fig. 7. Adsorption/desorption isotherms for sample Co/Mg/Alcal (a) and thermally treated at 923 K and reconstructed samples Co/Mg/AlW293 (b); Co/Mg/AlW352 (c); Co/Mg/AlN293 (d); Co/Mg/AlN353 (e).

The specific surface area of cobalt containing LDHs samples decreased upon reconstruction and calcination from  $170 \text{ m}^2 \text{ g}^{-1}$  for Co/Mg/Al<sub>cal</sub> to  $94 \text{ m}^2 \text{ g}^{-1}$  and  $131 \text{ m}^2 \text{ g}^{-1}$  for Co/Mg/Al<sub>W293</sub> and Co/Mg/Al<sub>W353</sub>, respectively. Thus, introduction of cobalt into Mg-Al-O mixed oxides lowered the specific surface area. Reformation medium had a considerable influence on the morphology of mixed metal oxides when nitrate solution provided higher specific surface area and higher pore volumes for the same reconstruction temperature. Moreover, a significant increase of specific surface area values were observed for the samples reconstructed in magnesium nitrate solution. Therefore, the better performance of Co/Mg/Al mixed oxides could be achieved [78].

### 3.2. Bi-substituted $Mg_3Al-CO_3$ layered double hydroxides

This part of PhD thesis is aimed at investigation of feasibility of preparation of LDH compounds with  $M^{III}=Bi$ . In order to minimise a possible effect of processing on the chemical composition of the resulting product, two independent methods were used to prepare LDH with the  $Mg_3Al_{1-x}Bi_x$  cation content ( $x = 0$  to 0.5), namely the conventional co-precipitation method and a formation via hydration of the mixed oxide powders in the carbonate-containing solutions. The powders were obtained either by calcination of the LDH (prepared by co-precipitation) or by using a novel alkoxide-free sol-gel method.

#### 3.2.1. Synthesis and characterization of $Mg_3Al_1$ and $Mg_3Al_{1-x}Bi_x$ LDHs produced via co-precipitation and aqueous sol-gel methods

The XRD patterns of non-substituted and bismuth-substituted Mg/Al/Bi LDH samples (Bi substitution level was from 0% to 50%) synthesized by co-precipitation method are shown in Fig. 8.

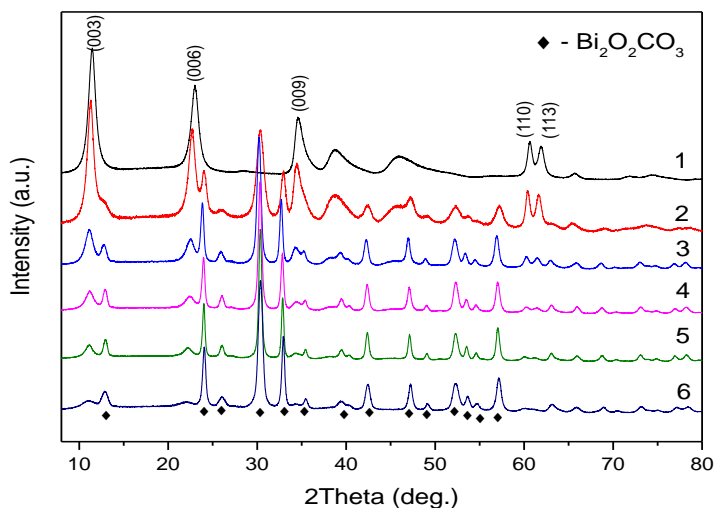


Fig. 8. XRD patterns of the LDH synthesis products obtained by co-precipitation method with the nominal  $Mg_3Al_{1-x}Bi_x$  cation composition:  $x = 0$  (1),  $x = 0.1$  (2),  $x = 0.2$  (3),  $x = 0.3$  (4),  $x = 0.4$  (5) and  $x = 0.5$  (6). The characteristic diffraction reflections of the LDH phase are indexed.

As seen, the XRD pattern of  $Mg_3Al_1$  LDH made by co-precipitation method is typical XRD pattern for the LDH showing the common features of layered materials, such as narrow, symmetric, strong lines at low  $2\theta$  values and weaker, less symmetric lines at high  $2\theta$  values. In the case of co-precipitation synthesis of Bi-substituted  $Mg_3Al_{1-x}Bi_x$  compounds, the diffraction lines of side phase  $Bi_2O_2CO_3$  along with Mg/Al/Bi LDH peaks are seen in the XRD patterns. With increasing substitutional level of bismuth, the intensities of the reflections of  $Bi_2O_2CO_3$  phase also monotonically increased and the peaks of Mg/Al/Bi phase became less intensive. Thus, the formation of layered structure becomes problematic when amount of bismuth exceed  $>20\%$ .

The SEM micrographs of as prepared by co-precipitation method bismuth-containing LDH, annealed at  $650^\circ C$  specimens and reconstructed LDH are shown in Fig. 9.

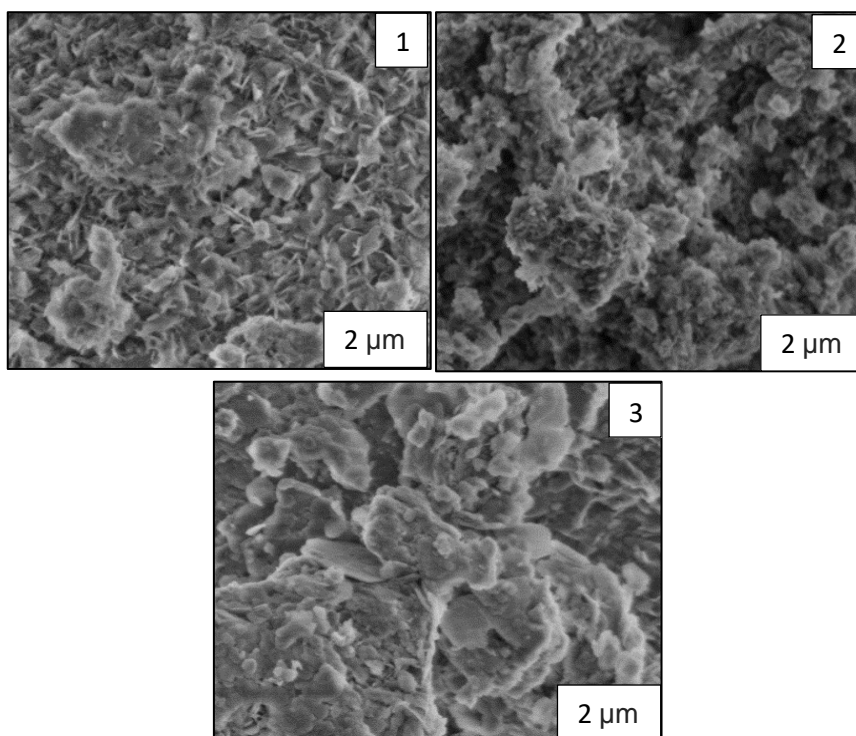


Fig. 9. SEM micrographs of  $Mg_3Al_{0.9}Bi_{0.1}$  synthesized by co-precipitation method: 1 - as prepared LDH, 2 – annealed at  $650^\circ C$  and 3- reconstructed LDH in water at  $80^\circ C$ .

The characteristic microstructure of synthesized LDH could be determined from the SEM micrograph. The formation of plate-like particles 0.5-2  $\mu\text{m}$  in size with hexagonal shape is evident. After calcination of Mg/Al/Bi LDH at 650°C the network of differently shaped particles varying in size from approximately have formed. The collapse of the LDH structure and appearance of porous mixed metal oxide structure was noticed. A layered double structure recovered after reconstruction procedure showed the formation of plate-like particles with more pronounced agglomeration. The particle size of LDH obtained after reconstruction remained almost the same.

### 3.2.2. Investigation of annealing temperature effect for sol-gel derived LDHs for successful reconstruction to layered structure

The XRD patterns of layered double hydroxides synthesized by sol-gel methods are shown in Fig. 10.

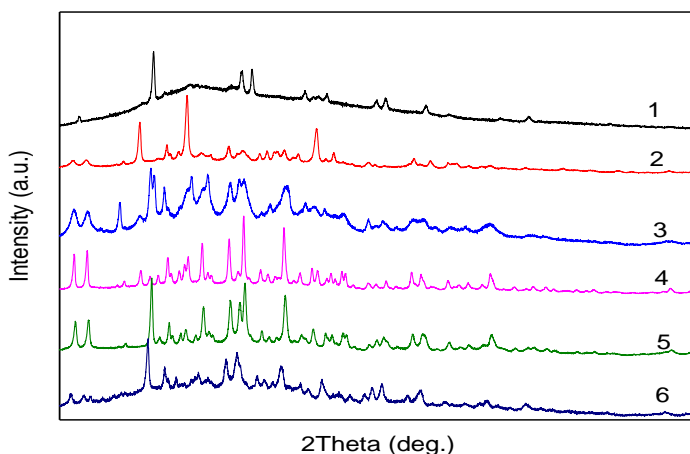


Fig. 10. XRD patterns of the LDH synthesis products obtained by sol-gel method with the nominal  $\text{Mg}_3\text{Al}_{1-x}\text{Bi}_x$  cation composition:  $x = 0$  (1),  $x = 0.1$  (2),  $x = 0.2$  (3),  $x = 0.3$  (4),  $x = 0.4$  (5) and  $x = 0.5$  (6).

The LDH obtained by sol-gel method, however, contains many organic impurities and shows very low crystallinity. Majority of the peaks are wide or being smudged and it is not possible to identify typical LDH peaks. These

results confirm that alkoxide-free sol-gel method is not suitable for the direct synthesis of layered double hydroxides. The Mg/Al/Bi LDH was not formed during the sol-gel processing.

The annealing temperature of LDH is very important because it is crucial for the successful reconstitution of the layered structure. The heat treatment of LDH should be performed at higher temperature than the temperature used for the destruction of double layers, but at lower temperature than the temperature suitable for the formation of spinel or another insoluble phase. The TG results showed that decomposition temperature of  $\text{Mg}_3\text{Al}_{0.5}\text{Bi}_{0.5}(\text{co-pr})$  and  $\text{Mg}_3\text{Al}_{0.5}\text{Bi}_{0.5}(\text{sg})$  samples should be around  $600^\circ\text{C}$  and  $500^\circ\text{C}$ , respectively. In Fig. 11, the XRD patterns of  $\text{Mg}_3\text{Al}_{1-x}\text{Bi}_x(\text{sg})$  samples annealed at  $650^\circ\text{C}$  are shown.

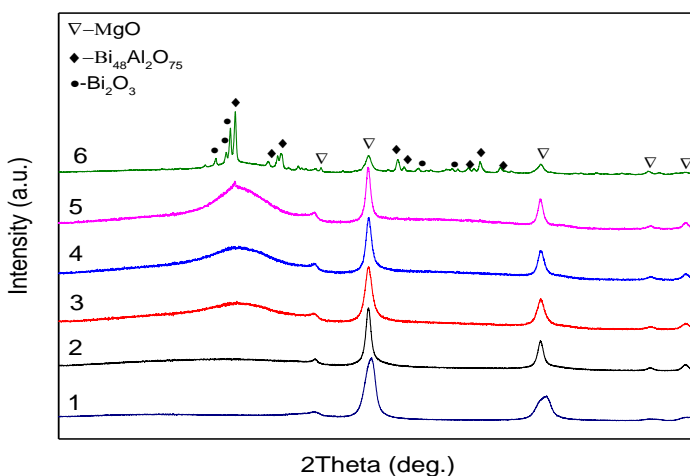


Fig. 11. XRD patterns of  $\text{Mg}_3\text{Al}_{1-x}\text{Bi}_x(\text{sg})$  samples annealed at  $650^\circ\text{C}$ :  $x=0$  (1),  $x=0.1$  (2),  $x=0.2$  (3),  $x=0.3$  (4),  $x=0.4$  (5) and  $x=0.5$  (6).

In comparison with co-precipitation method the MMO from sol-gel precursors have formed with higher crystallinity despite the LDH did not form during the sol-gel processing. Interestingly, with increasing amount of Bi all reflections are slightly moved to the higher  $2\theta$  angles. This is a consequence of incorporation of aluminium and bismuth in the framework of  $\text{Mg}(\text{Al})\text{O}$  or  $\text{Mg}(\text{AlBi})\text{O}$ , resulting in the formation of mixed-metal oxides [1].

### 3.2.3. Investigation of LDHs reformation process in water back to layered structure from mixed-metal oxides (“memory effect”)

The reformation process of LDH in water back to layered structure from mixed-metal oxides (“memory effect”) was also investigated. The XRD patterns of sol-gel derived LDH samples obtained after reconstruction process at 80 °C in water solution are given in Fig. 12.

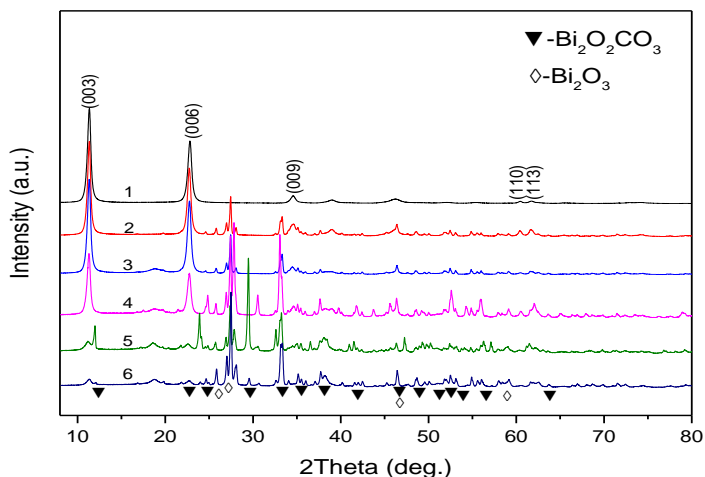


Fig. 12. XRD patterns of the products obtained after reconstruction of MMO powders prepared by sol-gel method. The nominal  $Mg_3Al_{1-x}Bi_x$  composition:  $x=0$  (1),  $x=0.1$  (2),  $x=0.2$  (3),  $x=0.3$  (4),  $x=0.4$  (5) and  $x=0.5$  (6).

MMO (mixed metal oxides) obtained from pure Mg/Al LDH and synthesized by sol-gel method were successfully reformed back to the layered structure. Intense and narrow diffraction peaks at 11° and 22°, ascribed to (003) and (006) planes, respectively, are clearly seen in both reconstructed Mg/Al LDH samples. As usually, asymmetric reflections (0kl) having different shape were obtained above 30° of  $2\theta$ . Reflections (110) and (113) noticed in 60°-62°  $2\theta$  confirm that reformation was completed fully. No peaks of low crystallinity of Mg(Al)O have been identified. During the reconstruction of sol-gel derived MMO when the amount of bismuth was about 10-30% only LDH and negligible amount of  $Bi_2O_3$  have formed during reformation process. With increasing amount of bismuth up to 40-50%, the predominant crystalline phase was  $Bi_2O_3CO_3$ . Thus, the term “reconstruction” we use to describe the reconstruction of sol-gel derived MMO is not correct.



In fact, this is a novel sol-gel synthesis approach developed for the fabrication of bismuth-containing LDH.

The surface morphology of sol-gel derived Mg-Al-Bi-O precursor (see Fig. 13) differs very much from typical microstructure of LDH.

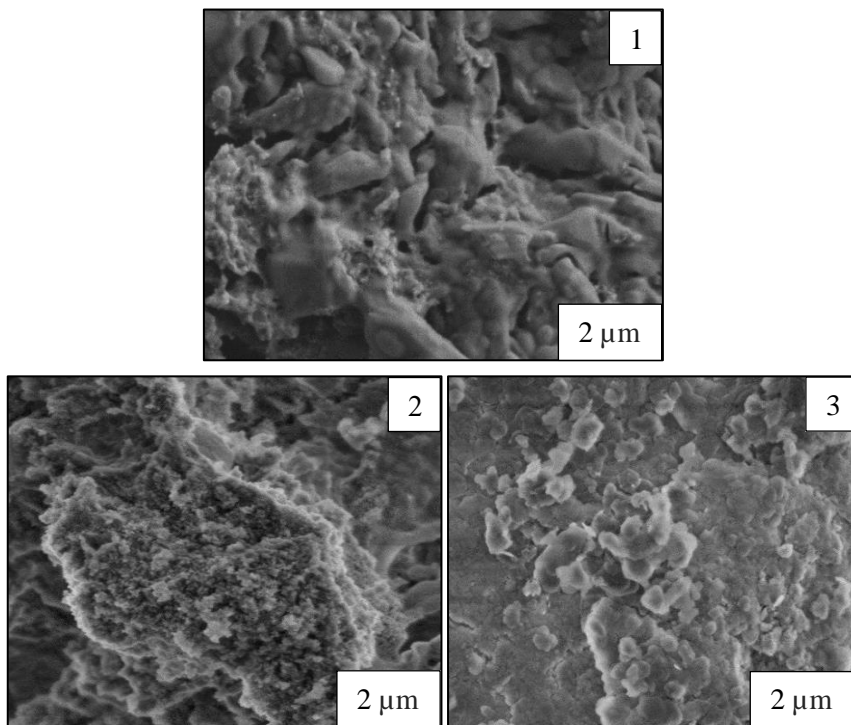


Fig. 13. SEM micrographs of  $\text{Mg}_3\text{Al}_{0.9}\text{Bi}_{0.1}$  synthesized by sol-gel method: 1- sol-gel precursor, 2 – annealed at  $650\text{ }^\circ\text{C}$ , 3- reconstructed (synthesized) LDH in water at  $80\text{ }^\circ\text{C}$ .

The representative SEM micrograph confirmed the formation of monolithic gel, in which individual particles were hardly distinguishable. On the other hand, the morphological features of the heat-treated sol-gel precursor at  $650^\circ\text{C}$  were almost identical to the MMO synthesized by co-precipitation method. The reconstruction method regenerated the metal hydroxide sheets and the plate-like geometry of the primary particles. Sol-gel derived Mg/Al/Bi LDH consist of the larger hexagonally shaped particles varying in size from approximately 200 to 500 nm. The good connectivity between the grains was observed. These nanograins showed tendency to form larger agglomerates.

Thus, the bismuth containing LDH  $Mg_3Al_{1-x}Bi_x$  ( $x \leq 0.2$ ) were prepared by low saturation co-precipitation method from carbonate-containing solutions and for the first time to the best of our knowledge the  $Mg_3Al_{1-x}Bi_x$  LDH were synthesized by an aqueous sol-gel processing. It was demonstrated that sol-gel method is not suitable for the direct synthesis of layered double hydroxides.

### 3.3. Dielectric properties of Bi-substituted LDHs synthesized by co-precipitation and sol-gel methods

The main aim of this part of doctoral dissertation was to compare dielectric properties of  $Mg_3Al_{1-x}Bi_x$  LDHs prepared by co-precipitation and sol-gel methods.

#### 3.3.1. Characterization of $Mg_3Al_{1-x}Bi_x$ LDH samples prepared via co-precipitation and aqueous sol-gel methods

The bismuth-substituted  $Mg_3Al_{1-x}Bi_x$  LDH samples ( $x$  was from 0% to 20%) were repeatedly synthesized by co-precipitation and sol-gel methods. Again, the XRD patterns of  $Mg_3Al_{1-x}Bi_x$  LDH samples obtained by co-precipitation method with introduction  $Bi^{3+}$  to the LDH structure showed formation of side phase  $Bi_2O_2CO_3$  along with  $Mg_3Al_{1-x}Bi_x$  LDHs. With increasing substitutional level of bismuth up to  $x = 0.2$  the intensity of the reflections of  $Mg_3Al_{1-x}Bi_x$  and  $Bi_2O_2CO_3$  phases decreased and increased, respectively. The XRD patterns of Bi-containing LDH samples obtained after reconstruction process of sol-gel derived mixed-metal oxides showed formation of negligible amount of  $Bi_2O_3$ . Lattice parameters  $a$  and  $c$  of synthesized LDH samples were calculated from XRD patterns. The obtained cell parameters of Mg/Al LDH prepared using co-precipitation ( $a = 3.051 \text{ \AA}$  and  $c = 23.192 \text{ \AA}$ ) and sol-gel ( $a = 3.059 \text{ \AA}$  and  $c = 23.388 \text{ \AA}$ ) methods are almost the same and are in a good agreement with literature data [1]. In the case of Mg/Al/Bi samples fabricated by both synthesis methods the both  $a$  and  $c$  parameters increased with increasing substitutional level of bismuth from  $a = 3.065 \text{ \AA}$  and  $c = 23.555 \text{ \AA}$  ( $Mg_3Al_{0.9}Bi_{0.1}$ ) to  $a = 3.074 \text{ \AA}$  and  $c = 23.829 \text{ \AA}$  ( $Mg_3Al_{0.8}Bi_{0.2}$ ) for co-precipitated samples and from  $a = 3.066 \text{ \AA}$  and  $c = 23.521 \text{ \AA}$  ( $Mg_3Al_{0.9}Bi_{0.1}$ ) to  $a = 3.068 \text{ \AA}$  and  $c = 23.908 \text{ \AA}$  ( $Mg_3Al_{0.8}Bi_{0.2}$ ) for sol-gel derived samples. This is not surprising, since the ionic radii of  $Bi^{3+}$

(1.03 Å) is much larger than  $\text{Al}^{3+}$  (0.535 Å). These XRD analysis results prove the existence of partial substitution of aluminium by bismuth in the LDH samples.

### 3.3.2. Investigation the temperature dependence of dielectric permittivity of $\text{Mg}_3\text{Al}_{1-x}\text{Bi}_x$ LDH samples prepared by different methods

It was previously determined for pure  $\text{Mg}_3\text{Al}_1$  LDH dry sample that at temperatures above 200 K Maxwell-Wagner relaxation could be observed [79]. At lower temperatures, very small losses were observed confirming the lack of conductivity in this material at studied frequencies. Temperature dependencies of real and imaginary parts of complex dielectric permittivity of  $\text{Mg}_3\text{Al}_{1-x}\text{Bi}_x$  LDH samples prepared by co-precipitation method are shown in Fig. 14.

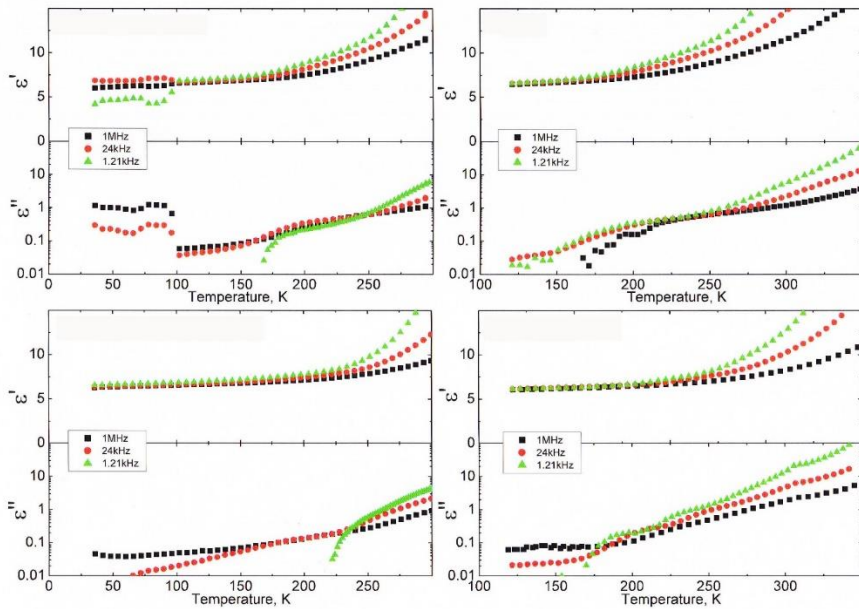


Fig. 14. Temperature dependencies of real ( $\epsilon'$ ) and imaginary ( $\epsilon''$ ) parts of complex dielectric permittivity of  $\text{Mg}_3\text{Al}_{0.9}\text{Bi}_{0.1}$  (top) and  $\text{Mg}_3\text{Al}_{0.8}\text{Bi}_{0.2}$  (bottom) LDH samples prepared by co-precipitation method. The results for vacuumed samples are presented at left.

The real part of complex permittivity ( $\epsilon'$ ) is almost constant (5.5–6.5) for vacuumed and non-vacuumed samples. Only non-vacuumed  $\text{Mg}_3\text{Al}_{0.9}\text{Bi}_{0.1}$  sample shows frequency dispersion at higher temperature ( $>200$  K). The dispersion can be explained on the basis of complex structure of synthesized LDH having bismuth as dopant that forms intrinsic electric moments [80]. Both parts of the complex dielectric permittivity decreased with increasing measurement frequency. The temperature dependence of real and imaginary parts of complex dielectric permittivity of  $\text{Mg}_3\text{Al}_{0.9}\text{Bi}_{0.1}$  LDH sample prepared by sol-gel method is very similar (see Fig. 15).

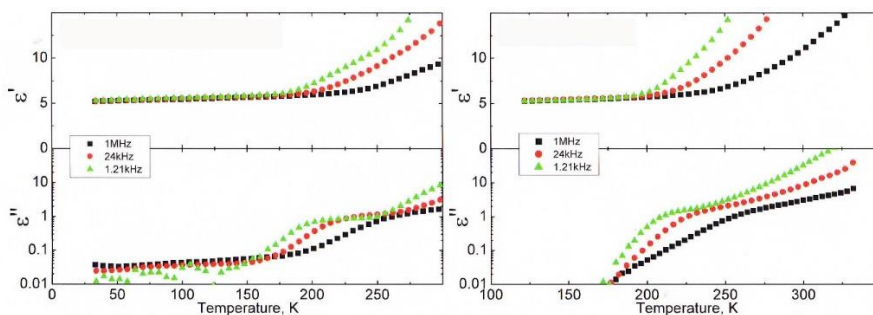


Fig. 15. Temperature dependencies of real ( $\epsilon'$ ) and imaginary ( $\epsilon''$ ) parts of complex dielectric permittivity of  $\text{Mg}_3\text{Al}_{0.9}\text{Bi}_{0.1}$  LDH prepared by sol-gel method. The results for vacuumed samples are presented at left.

The increase in  $\epsilon'$  is more pronounced at higher temperatures and at lower frequencies for non-vacuumed sample. This may be due to the frequency dependent orientational polarization [81]. Evidently, the dielectric properties of  $\text{Mg}_3\text{Al}_{1-x}\text{Bi}_x$  LDH samples do not depend on surface morphology, consequently on the preparation technique [82]. The structural transition were not observed, however, for all bismuth-doped LDH samples [83, 84]. Moreover, the increase of  $\epsilon'$  with increasing temperature indicates the semiconducting behaviour of our  $\text{Mg}_3\text{Al}_{1-x}\text{Bi}_x$  LDH samples [85].

In conclusion, the temperature dependence of dielectric permittivity of  $\text{Mg}_3\text{Al}_{1-x}\text{Bi}_x$  LDH samples prepared by different methods was investigated. In general, the increase in  $\epsilon'$  was more pronounced at higher temperatures and at lower frequencies for non-vacuumed samples. The dielectric properties were independent on surface morphology of  $\text{Mg}_3\text{Al}_{1-x}\text{Bi}_x$  LDH samples fabricated by two different synthesis routes. Finally, no structural transitions were observed for all bismuth-doped LDH samples. The real part of complex

permittivity ( $\epsilon'$ ) is almost constant (5.5–6.5) for  $\text{Mg}_3\text{Al}_{1-x}\text{Bi}_x$  LDH samples prepared by co-precipitation method, however, slightly depends on the amount of Bi for the sol-gel derived  $\text{Mg}_3\text{Al}_{1-x}\text{Bi}_x$  LDH samples.

### 3.4. Sonication accelerated formation of Mg-Al-phosphate layered double hydroxide via sol-gel prepared mixed metal oxides

The main aim of this part of doctoral dissertation was to combine the aqueous sol-gel based method of production of  $\text{Mg}_2\text{Al-OH}$  LDH followed by the intercalation with phosphate anion via the successive anion exchange reactions,  $\text{OH}^- \rightarrow \text{Cl}^-$  and  $\text{Cl}^- \rightarrow \text{H}_2\text{PO}_4^-$ , with high-power sonication, and to demonstrate that the application of a kW-level ultrasound considerably accelerates all stages of the final product formation, namely hydration and both anion exchanges.

#### 3.4.1 Temperature and high-power ultrasound effect on $\text{Mg}_2\text{Al}_{(\text{MMO})}$ hydration

Experimentally it was found that formation of LDH phase by hydration of  $\text{Mg}_2\text{Al}_{(\text{MMO})}$  at room temperature is rather slow, even after 24 h, the diffraction reflections of the LDH phase are still wide which suggests a small average crystallite size and a broad size distribution. Therefore, the reaction temperature was increased up to 80°C. A single-phase  $\text{Mg}_2\text{Al-OH}$  LDH was obtained after 2 h hydration of  $\text{Mg}_2\text{Al}_{(\text{MMO})}$  (Fig. 16). In the third set of experiments, high-power ultrasound was applied to prepare LDHs of the same composition. It was found that the sonication assisted reaction occurs faster in comparison with reaction performed at 80°C under vigorous mechanical stirring. A single phase  $\text{Mg}_2\text{Al-OH}$  LDH was obtained already after 30 min of ultrasound treatment (Fig. 17). Moreover, in the case of the sonication assisted reaction, the LDH, as the main phase, appeared already after 2-min treatment; however, the hydration was still uncomplete: traces of the MMO precursor were present in the product even after 15 min of hydration. It was observed from the comparison of the FWHM values of the basal reflections of the LDH phases crystallized either at room temperature or at 80°C or under applied high-power ultrasound that the reaction rate increased by more than factor of 20 (Fig. 18).

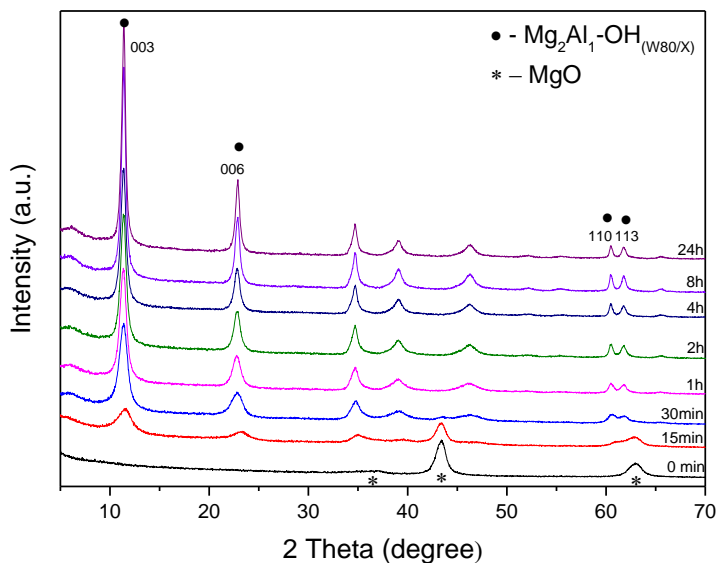


Fig. 16. XRD patterns of the  $\text{Mg}_2\text{Al}_1\text{-OH}_{(\text{W}80/\text{X})}$  LDH products obtained after reconstruction of  $\text{Mg}_2\text{Al}_1(\text{MMO})$  in water at 80 °C using different synthesis time.

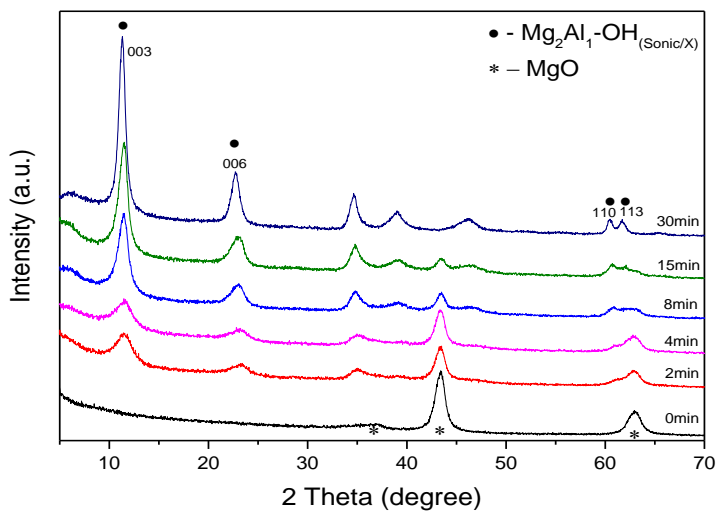


Fig. 17. XRD patterns of the  $\text{Mg}_2\text{Al}_1\text{-OH}_{(\text{Sonic}/\text{X})}$  LDH products obtained after reconstruction of  $\text{Mg}_2\text{Al}_1(\text{MMO})$  in water using different synthesis (sonication) time.

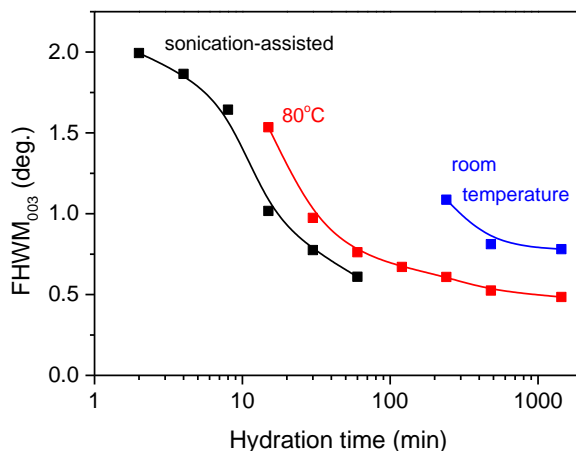


Fig. 18. The full width at half maximum (FWHM) values of the 003 basal diffraction peaks of LDH phase obtained by hydration of  $Mg_2Al$  MMO either at room temperature or at  $80^\circ C$  or under applied high-power ultrasound as a function of hydration time. Notice the logarithmic time scale.

### 3.4.2 High-power ultrasound effect on LDH interlayer substitution, composition and morphology

A hydroxide-to-phosphate direct anion exchange was unsuccessful. Therefore, a two-step hydroxide  $\rightarrow$  chloride  $\rightarrow$  phosphate process was attempted. Due to a small difference in size of  $OH^-$  and  $Cl^-$ , the shift in the basal diffraction reflections to lower  $2\theta$  angles was also rather small (Fig. 19). The  $Cl^-$ -intercalation reaction at room temperature was found to take 15 min, while the sonication assisted anion exchange was completed in 4 min. The chloride-to-phosphate anion exchange was manifested in the shift of the basal reflections in the XRD patterns towards lower  $2\theta$  angles indicating a considerable increase of the interlayer distance. The anion exchange took about 30 min in the case of standard mixing procedure at room temperature, while the exchange was complete in 4 min when the high-power ultrasound was applied. The broader reflections were observed in the XRD patterns of  $Mg_2Al-H_xPO_4$  LDHs (Fig. 19) in comparison with those seen in the patterns of the hydroxide-intercalated and chloride-intercalated LDHs. This can indicate some disorder in arrangement of the phosphate anions in the interlayer.

The lattice parameters  $a$  ( $a = 2d_{(110)}$ ) and  $c$  ( $c = 3d$ ) calculations for all the obtained LDHs are listed in Table 3 [1]. The maximum absolute errors in determination of the parameters  $c$  and  $a$  were  $0.15 \text{ \AA}$  and  $0.01 \text{ \AA}$ , respectively. The  $a$ -parameter values of the obtained  $\text{Mg}_2\text{Al}$  LDHs intercalated with either hydroxide, chloride or phosphate are equal within the experimental error. The difference between the  $c$ -parameter values of the respective  $\text{Mg}_2\text{Al-OH}$  and  $\text{Mg}_2\text{Al-Cl}$  LDHs is in good agreement with the previously reported data [3] and the references therein (about  $0.4\text{-}0.6 \text{ \AA}$ ).

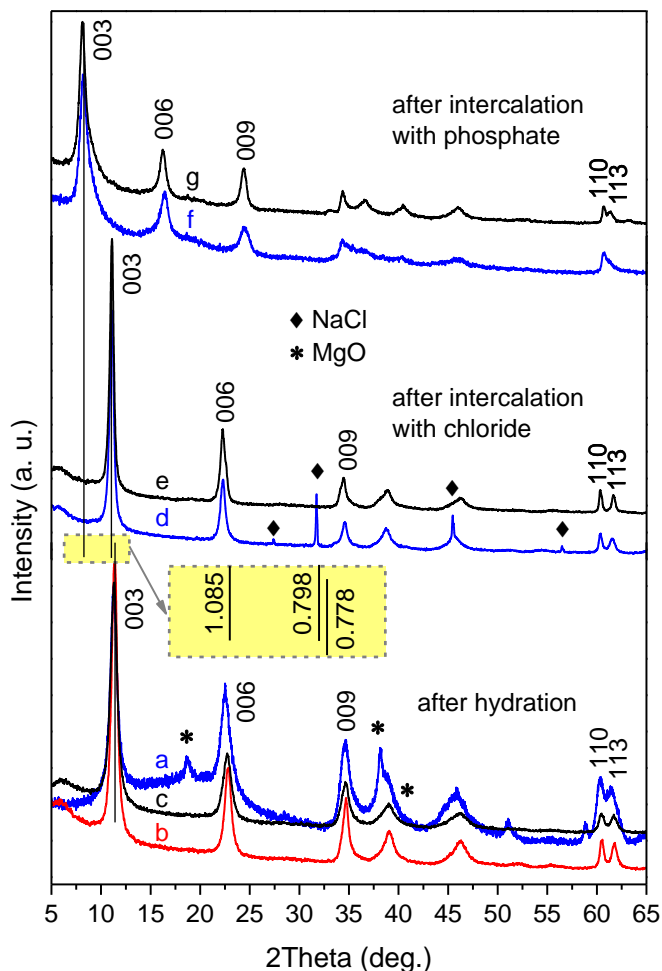


Fig. 19. Typical XRD patterns of the products obtained after hydration of MMO resulted in formation of  $\text{Mg}_2\text{Al-OH}$  LDH (a, b and c) and subsequent hydroxide-to-chloride (e, d) and chloride-to-phosphate (f, g) anion exchanges



conducted in different conditions: (a) at room temperature for 24 h -  $\text{Mg}_2\text{Al-OH}_{(25^\circ\text{C}/24\text{h})}$ , (b) at  $80^\circ\text{C}$  for 2 h -  $\text{Mg}_2\text{Al-OH}_{(80^\circ\text{C}/2\text{h})}$  (c) with ultrasound applied for 30 min -  $\text{Mg}_2\text{Al-OH}_{(\text{Sonic}/30\text{min})}$ , (d) at room temperature for 15 min -  $\text{Mg}_2\text{Al-Cl}_{(25^\circ\text{C}/15\text{min})}$ , (e) with ultrasound applied for 4 min -  $\text{Mg}_2\text{Al-Cl}_{(\text{Sonic}/4\text{min})}$ , (f) at room temperature for 1 h -  $\text{Mg}_2\text{Al-H}_x\text{PO}_4$  ( $25^\circ\text{C}/1\text{h}$ ) and (g) with ultrasound applied for 8 min -  $\text{Mg}_2\text{Al-H}_x\text{PO}_4$  ( $\text{Sonic}/8\text{min}$ ). Inset: basal spacing values (in nm) of the respective LDH phases

The obtained LDHs were analysed using ICP-OES. It was determined that the stoichiometry of magnesium and aluminium in the sol-gel derived  $\text{Mg}_2\text{Al}$  LDHs is close to the nominal one regardless of the methods used for acceleration of the hydration and the anion-exchanges. The Mg/Al/P ratio in the phosphate-intercalated LDHs is close to 2/1/1. Taking into account the generic formula of the  $\text{M}^{\text{II}}\text{-M}^{\text{III}}$  LDH (see Introduction), the obtained ratio indicates the type of the intercalated phosphate anion, namely dihydrogen phosphate,  $\text{H}_2\text{PO}_4^-$ . The chemical composition of the phosphate-intercalated LDH produced in this work can be represented as  $\text{Mg}_{0.67}\text{Al}_{0.33}(\text{OH})_2(\text{H}_2\text{PO}_4)_{0.33}\cdot z\text{H}_2\text{O}$ .

Table 3. The interplanar distances used for calculation and the calculated lattice parameters ( $a$ ,  $c$ ) of the LDHs obtained via hydration and anion exchanges.

Sample ID	$d_{(003)}$ , Å	$d_{(006)}$ , Å	$d_{(110)}$ , Å	$c$ , Å	$a$ , Å
$\text{Mg}_2\text{Al-OH}_{(80^\circ\text{C}/2\text{h})}$	7.843	3.906	1.532	23.483	3.064
$\text{Mg}_2\text{Al-OH}_{(\text{Sonic}/30\text{min})}$	7.908	3.930	1.536	23.652	3.070
$\text{Mg}_2\text{Al-Cl}_{(25^\circ\text{C}/15\text{min})}$	7.986	3.985	1.534	23.934	3.068
$\text{Mg}_2\text{Al-Cl}_{(\text{Sonic}/4\text{min})}$	8.004	3.993	1.527	23.985	3.054
$\text{Mg}_2\text{Al-H}_x\text{PO}_4$ ( $25^\circ\text{C}/1\text{h}$ )	9.992	5.277	1.523	30.819	3.049
$\text{Mg}_2\text{Al-H}_x\text{PO}_4$ ( $\text{Sonic}/8\text{min}$ )	10.779	5.380	1.525	32.309	3.050

After lattice parameters calculation, the observed variation in the values of parameter  $c$  of the LDHs intercalated with phosphate (Table 3) may imply several possibilities of arrangement of phosphate anion. Using the Table 3 data and taking into account the thickness of the Mg-Al hydroxide layer ( $d_0=4.77$  Å [86]), the calculated interlayer gallery height is 6.00 Å and 5.30 Å for

$\text{Mg}_2\text{Al-H}_x\text{PO}_4$  (Sonic/30min) and  $\text{Mg}_2\text{Al-H}_x\text{PO}_4$  (25°C/1h) LDHs respectively. This data give possibility to model the arrangement of phosphate anion similar to that reported in Ref [87] for the pyrovanadate-intercalated  $\text{Zn}_2\text{Al}$  LDH. Calculations showed that the most probable orientation of the phosphate anion is the following: a tetrahedron edge is perpendicular to the hydroxide layer (Fig. 20).

The surface morphology of the prepared LDH samples was investigated by SEM and STEM. The SEM micrographs are shown in Fig. 21. The particles agglomerated of flake-like crystallites were observed in all samples. The STEM micrographs (Fig. 22) reveal characteristic hexagonal shape of the flake-like LDH crystallites. It should be stressed here that no effect of the preparation conditions (increase of temperature, application of ultrasound) on size and shape of LDH particles nor crystallites has been observed.

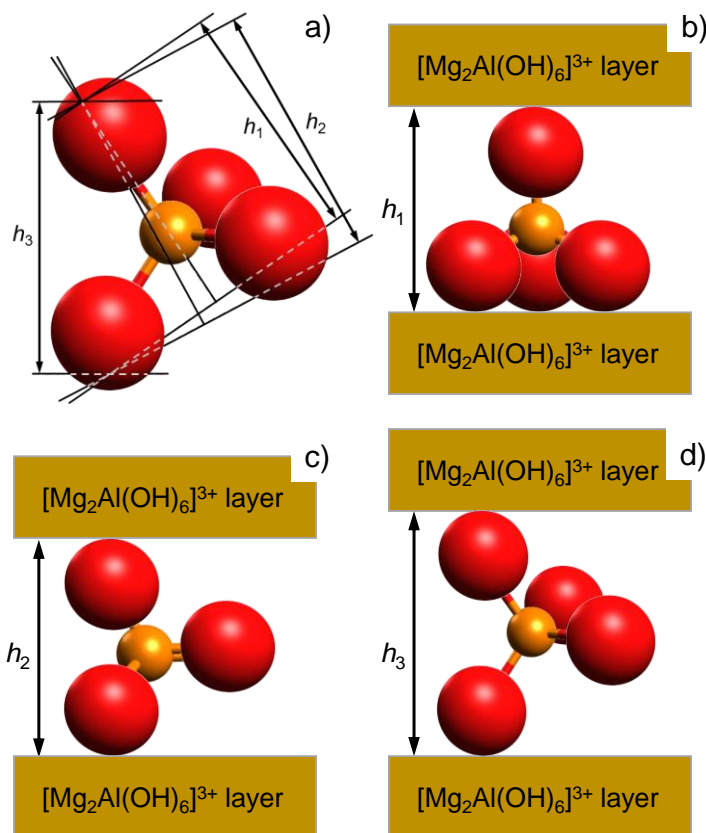


Fig. 20. Schematic representations of (a) the most characteristic dimensions of  $\text{H}_x\text{PO}_4^{(3-x)-}$  anion and the respective orientations of the anion in the  $\text{Mg}_2\text{Al}$

LDH interlayer: (b) the space height of the tetrahedron is perpendicular to the hydroxide layer, (c) the height of triangular face of the tetrahedron is perpendicular to the hydroxide layer, and (d) edge length of the tetrahedron is perpendicular to the hydroxide layer. Hydrogen ions are not shown

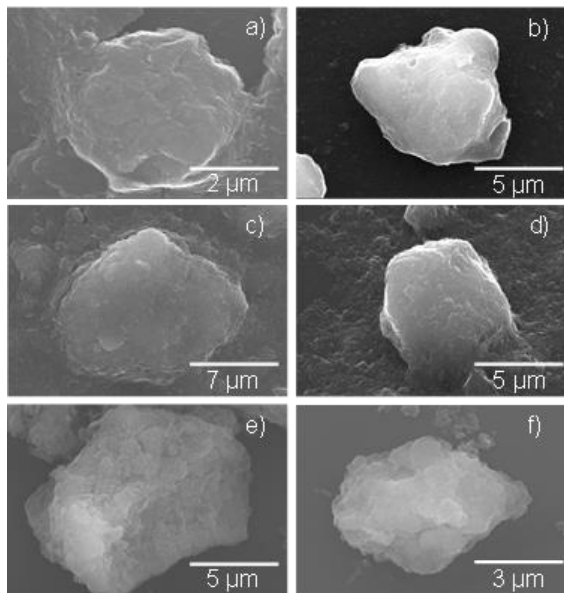


Fig. 21. SEM micrographs of the LDH powders prepared via hydration of MMO followed by anion exchanges at different temperatures without and with application of high-power ultrasound: (a)  $\text{Mg}_2\text{Al-OH}_{(80^\circ\text{C}/24\text{h})}$ , (b)  $\text{Mg}_2\text{Al-OH}_{(\text{Sonic}/30\text{min})}$ , (c)  $\text{Mg}_2\text{Al-Cl}_{(25^\circ\text{C}/15\text{min})}$ , (d)  $\text{Mg}_2\text{Al-Cl}_{(\text{Sonic}/4\text{min})}$ , (e)  $\text{Mg}_2\text{Al-H}_2\text{PO}_4_{(25^\circ\text{C}/1\text{h})}$  and (f)  $\text{Mg}_2\text{Al-H}_2\text{PO}_4_{(\text{Sonic}/8\text{min})}$

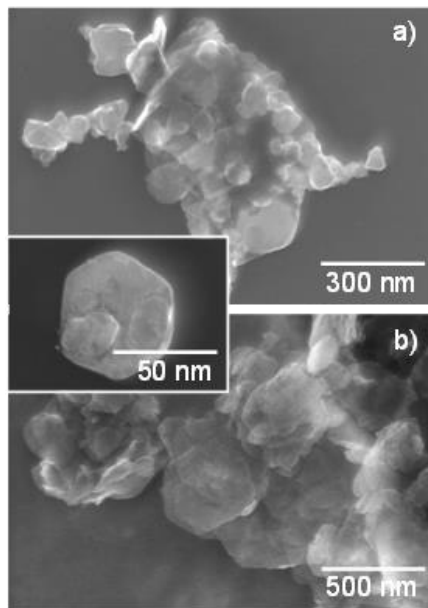


Fig. 22. STEM micrographs of the LDHs obtained via sonication-assisted hydration and anion exchanges: (a)  $\text{Mg}_2\text{Al-Cl}_{(\text{Sonic}/4\text{min})}$  and (b)  $\text{Mg}_2\text{Al-H}_2\text{PO}_4_{(\text{Sonic}/8\text{min})}$ . Inset shows a detached crystallite of  $\text{Mg}_2\text{Al-OH}_{(\text{Sonic}/30\text{min})}$  LDH

In conclusion, applied procedure of the formation of LDH intercalated with hydroxide via hydration of sol-gel prepared MMO followed by the deintercalation of  $\text{OH}^-$  and the intercalation with phosphate via a two-step anion exchange appears to be a promising way for production of stoichiometric LDH intercalated with functional species. High-power sonication considerably accelerates the formation of LDH phase from mixed metal oxides and the successive anion exchange processes.

### 3.5. Cast iron corrosion protection with chemically modified $\text{Mg}_2\text{Al}_1$ layered double hydroxides synthesized using a novel approach

The main objectives of this part of doctoral dissertation were to study the corrosion protection functionality of the layered double hydroxides synthesized using a novel approach, including LDHs whose metal hydroxide layers were modified with cerium, and to monitor anion release from these LDH in NaCl solutions and their corrosion inhibitive action on cast iron samples by electrochemical impedance spectroscopy.

### 3.5.1. Analysis and characterization of synthesized and substituted $\text{Mg}_2\text{Al}_1$ and $\text{Mg}_2\text{Al}_{0.9}\text{Ce}_{0.1}$ LDHs

XRD patterns of  $\text{Mg}(2)\text{Al-OH}$  and  $\text{Mg}(2)\text{Al-10\%Ce-OH}$  layered double hydroxide powders from the high-power sonication assisted synthesis and of successive anion exchanges, are shown in Fig. 23. The XRD patterns of the compositions obtained as a result of the anion exchanges demonstrated a regular shift of the diffraction peaks of the (00 $l$ ) family towards lower angles indicating that the hydroxide-to-chloride and chloride-to-phosphate substitutions were complete.

Lattice parameters  $a$  ( $a = 2d_{(110)}$ ) and  $c$  ( $c = 3/2[d_{(003)} + 2d_{(006)}]$ ) of the obtained LDH were calculated using the inter-planar distances corresponded to the angular positions of the diffraction peaks (003), (006) and (110) were listed in Table 4 [1]. Basal spacing was calculated as  $d=c/3$ , and the interlayer height (gallery height,  $h$ ) was found by subtracting the hydroxide layer thickness from the basal spacing value. The  $\text{Mg}(2)\text{Al}$  hydroxide layer thickness was considered to be 0.477 nm [86]. The  $h$ -value estimated for  $\text{Mg}(2)\text{Al-H}_2\text{PO}_4$  suggested that the phosphate anion was arranged in a such way that a line along its maximum dimension was perpendicular to the layer plane [88].

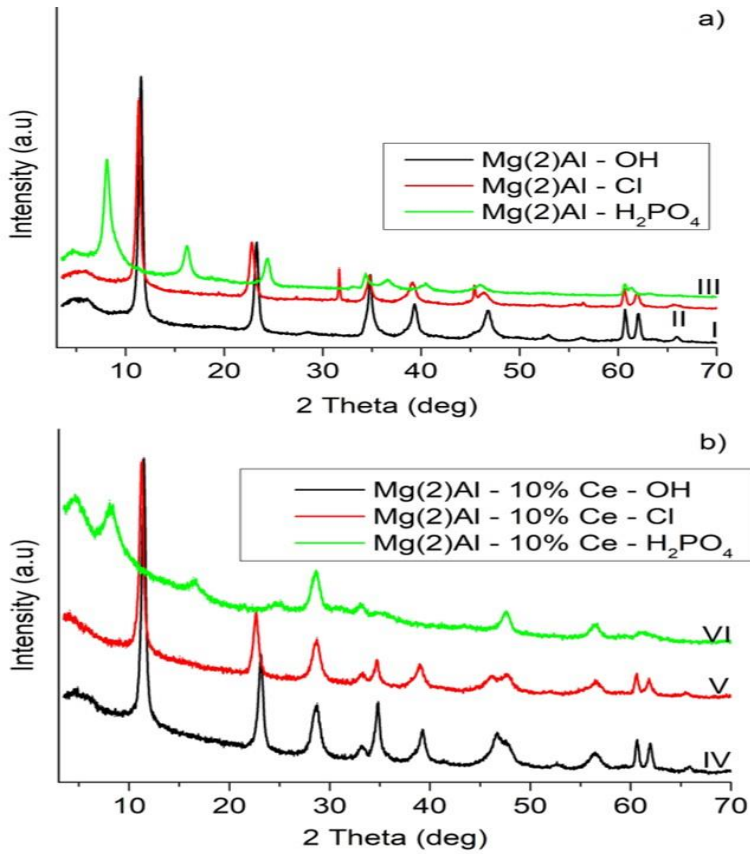


Fig. 23. XRD patterns of the compositions produced by hydration of the sol-gel prepared mixed metal oxides followed by two-step (hydroxide-to-chloride and chloride-to-phosphate) anion exchange: a) - Mg(2)Al-OH (I), Mg(2)Al-Cl (II), and Mg(2)Al-H<sub>2</sub>PO<sub>4</sub> (III); b) - Mg(2)Al-10%Ce-OH (IV), Mg(2)Al-10%Ce-Cl (V), and Mg(2)Al-10%Ce-H<sub>2</sub>PO<sub>4</sub> (VI).

Table 4. The lattice parameters ( $a$ ,  $c$ ) and basal spacings ( $d$ ) for the LDH compositions intercalated with different anions.

<b>Composition</b>	<b><math>c</math>, nm</b>	<b><math>a</math>, nm</b>	<b><math>d</math>, nm</b>
Mg(2)Al-OH	2.2950	0.3049	0.7650
Mg(2)Al-Cl	2.3426	0.3052	0.7808
Mg(2)Al-H <sub>2</sub> PO <sub>4</sub>	3.2662	0.3051	1.0887
Mg(2)Al-10%Ce-OH	2.3100	0.3052	0.7700
Mg(2)Al-10%Ce-Cl	2.3565	0.3052	0.7855
Mg(2)Al-10%Ce-H <sub>2</sub> PO <sub>4</sub>	3.2945	0.3054	1.0981

The lattice parameters values of cerium-substituted LDH compositions were found to be regularly higher than the corresponding values of Mg(2)Al LDH intercalated with the same anions (see Table 4). This reflects the increase of the hydroxide layer thickness caused by a partial substitution of Al<sup>3+</sup> by a larger sized Ce<sup>3+</sup>.

STEM images of particles/crystallites of Mg(2)Al-OH and Mg(2)Al-10%Ce-OH LDH obtained with or without the ultrasound treatment are shown in Fig. 24.

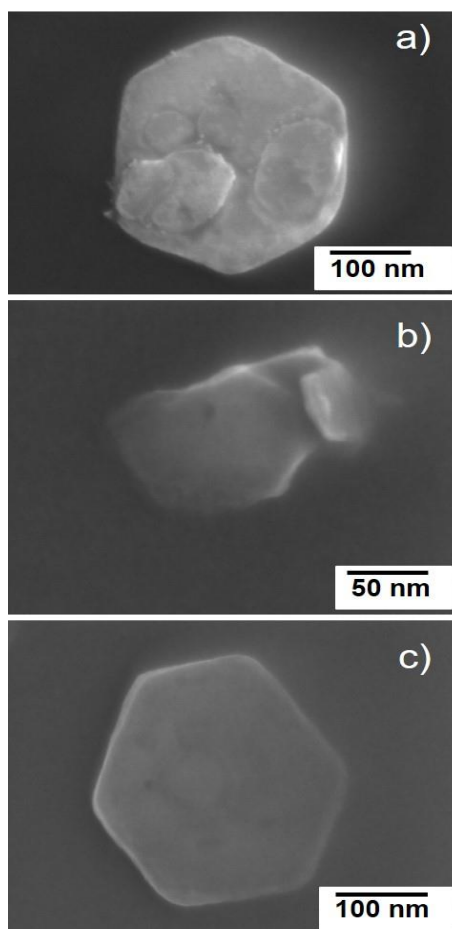


Fig. 14. STEM images of fully dispersed LDH particles/crystallites: a) -  $\text{Mg(2)Al-OH}$  produced by hydration of the sol-gel prepared mixed metal oxides without high-power sonication, b) and c) -  $\text{Mg(2)Al-OH}$  and  $\text{Mg(2)Al-10\%Ce-OH}$ , respectively, produced by sonication-assisted hydration of the sol-gel prepared mixed metal oxides.

In all the above-mentioned cases, hexagonal flake-shaped crystallites inherent to the layered double hydroxides were observed. The characteristic size (diameter) of the flakes was estimated to range from 50 to 150 nm. Based on comparative analysis of series of the STEM images, we concluded that the high-power sonication did not impact either size or shape of the LDH crystallites, but, the crystallites of LDH produced with application of ultrasounds were found to be less agglomerated.



### 3.5.2. Effect of LDHs to Electrochemical characterization and corrosion protection

Initially, the cast iron substrates were immersed in two test solutions (50 mM NaCl and 50 mM NaCl + 5 mM Na<sub>2</sub>HPO<sub>4</sub>) as described in *Experimental* to reveal the effect of phosphate anions on the sample surface in a corrosive media. Fig. 25 shows the EIS spectra acquired after 2 to 168 h of immersion in the solutions.

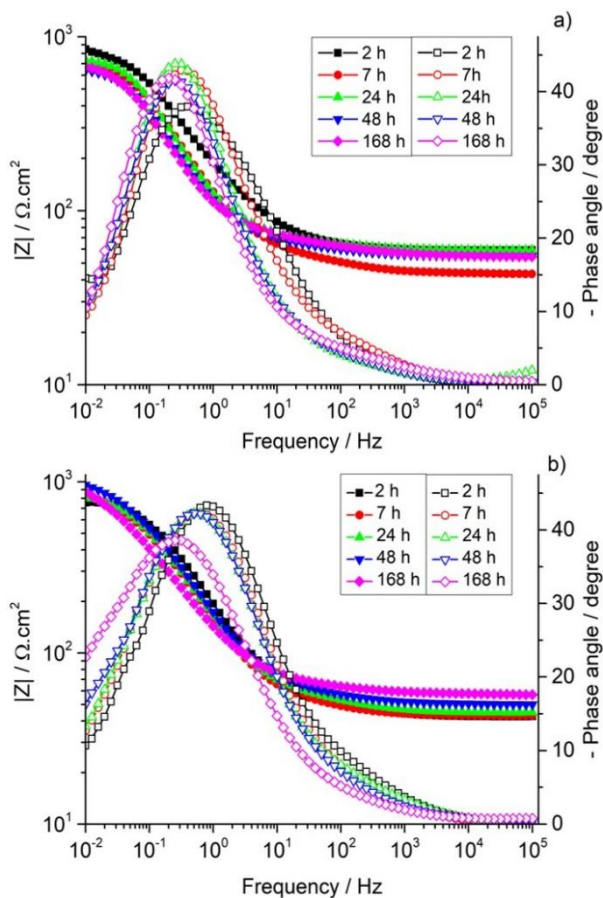


Fig. 25. EIS spectra for the cast iron substrate immersed a) in a 50 mM NaCl solution and b) in a 50 mM NaCl + 5 mM Na<sub>2</sub>HPO<sub>4</sub> solution (Solid symbols denote the total impedance, empty symbols denote the phase angle).

Total impedance ( $|Z|$ ) at relevant frequencies is the main parameter used for corrosion activity assessment in all studied substrate-solution systems. It has been observed that the impedance decreased immediately after the first minute of immersion of the iron substrate in the 50 mM NaCl solution. The values of impedance observed in the spectra in Fig. 25a suggest the formation of corrosion products on the surface of the sample, justifying the slow decrease of low frequency impedance through the 168 h of measurement.

When the sample is immersed in the solution containing  $\text{Na}_2\text{HPO}_4$  (Fig. 25b) the impedance values is stable at least during 24 h. After this period of time, due to oxide formation and deposition of phosphate on the substrate, the values of  $|Z|$  increased again; however, a part of the sample was kept protected even after one week of immersion.

The images of the cast iron substrates immersed for one week in a NaCl solution either with or without the corrosion inhibitive species are shown in Fig. 26.

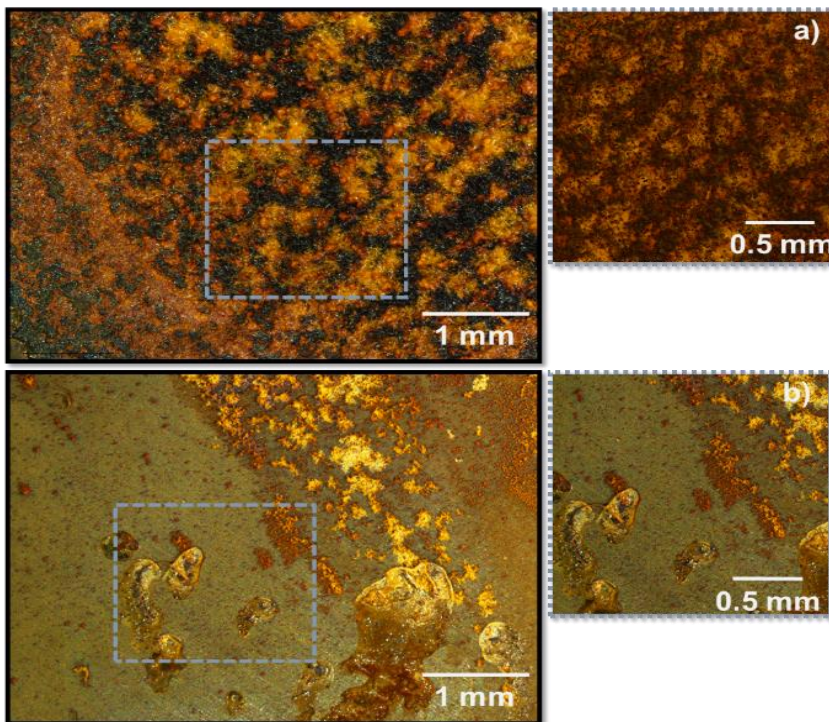


Fig. 26. The cast iron substrates after 1-week immersion a) in a 50 mM NaCl solution and b) in a 50 mM NaCl + 5 mM  $\text{Na}_2\text{HPO}_4$  solution.

Images in Fig. 26 indicate that phosphate species are effective for corrosion protection of cast iron when introduced in the 50 mM NaCl solution. The presence of corrosion signs (pitting corrosion) on the surface of the sample in Fig. 26b can be explained by the insufficient amount of phosphate species (5 mM Na<sub>2</sub>HPO<sub>4</sub> in a 50 mM NaCl solution) to protect the entire surface.

The next step of the study was an immersion test using the inhibitive species intercalated into the LDH produced using the novel approach, Mg(2)Al-H<sub>2</sub>PO<sub>4</sub>. The same test was also performed in the solution containing Mg(2)Al-OH for comparison. Fig. 27 shows the EIS spectra acquired after 2 to 168 h of immersion in the respective solutions.

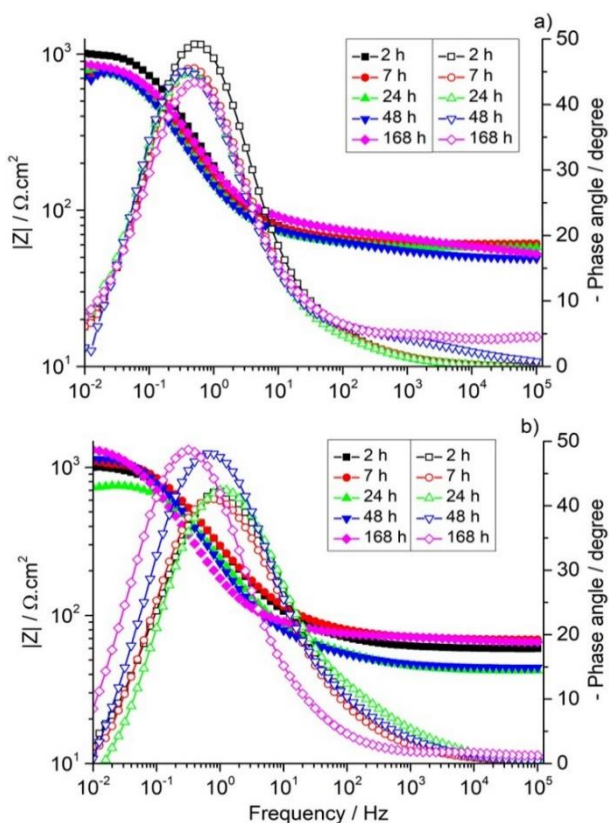


Fig. 27. EIS spectra for the cast iron substrate immersed in solutions containing the layered double hydroxides a) 50 mM NaCl + 5 mM Mg(2)Al-OH and b) 50 mM NaCl + 5 mM Mg(2)Al-H<sub>2</sub>PO<sub>4</sub>. (Solid symbols denote the total impedance, empty symbols denote the phase angle).

Mg(2)Al-OH layered double hydroxide in a NaCl solution releases OH<sup>-</sup> and traps Cl<sup>-</sup> increasing the pH to 12. Since hydroxide anion has no corrosion inhibitive ability, the impedance values slowly decrease until formation of iron oxide (Fig. 27a). After about 48 h of immersion, the hydroxide-to-chloride anion exchange reaction seems to be completed and the local decrease of chloride ions causes partial protection of the cast iron (the plot at 168 h).

Figure 27b shows a gradual increase of the impedance after 24 h and until one-week immersion in a 50 mM NaCl + 5 mM Mg(2)Al-H<sub>2</sub>PO<sub>4</sub> solution that indicates the effective anticorrosion performance of the Mg(2)Al-H<sub>2</sub>PO<sub>4</sub> LDH as a nanocontainer of inhibitive species that releases H<sub>2</sub>PO<sub>4</sub><sup>-</sup> and captures Cl<sup>-</sup>. The final aspect of the sample (Fig. 28) with less pitting corrosion in the surface was better than the one after the same time of immersion in a 50 mM NaCl + 5 mM Na<sub>2</sub>HPO<sub>4</sub> solution (Fig. 26b) although the amounts of phosphates in both tests were the same.

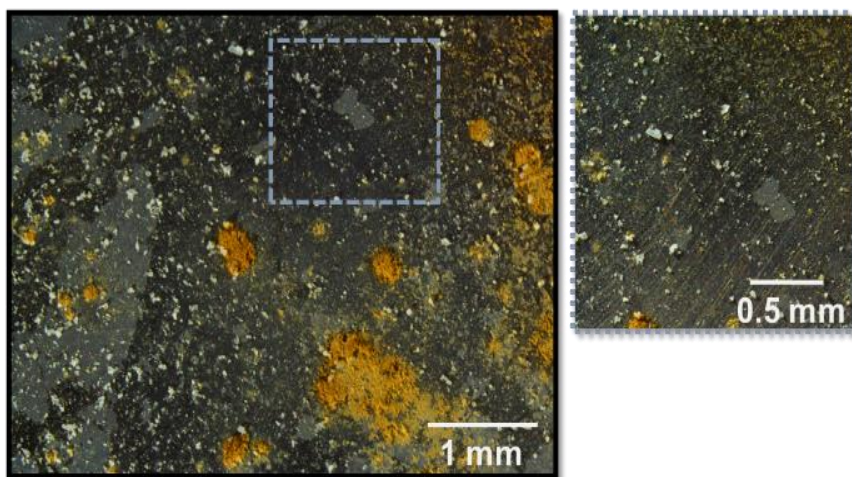


Fig. 28. The cast iron substrate after a 1-week immersion in a 50 mM NaCl solution with addition of 5 mM Mg(2)Al-H<sub>2</sub>PO<sub>4</sub> LDH.

To support the results obtained from the immersion test, an XRD study of the corrosion products collected from the surface of the samples after 1-week

immersion was performed. Figure 29 shows the XRD patterns of the products precipitated/formed on the surface of each cast iron sample.

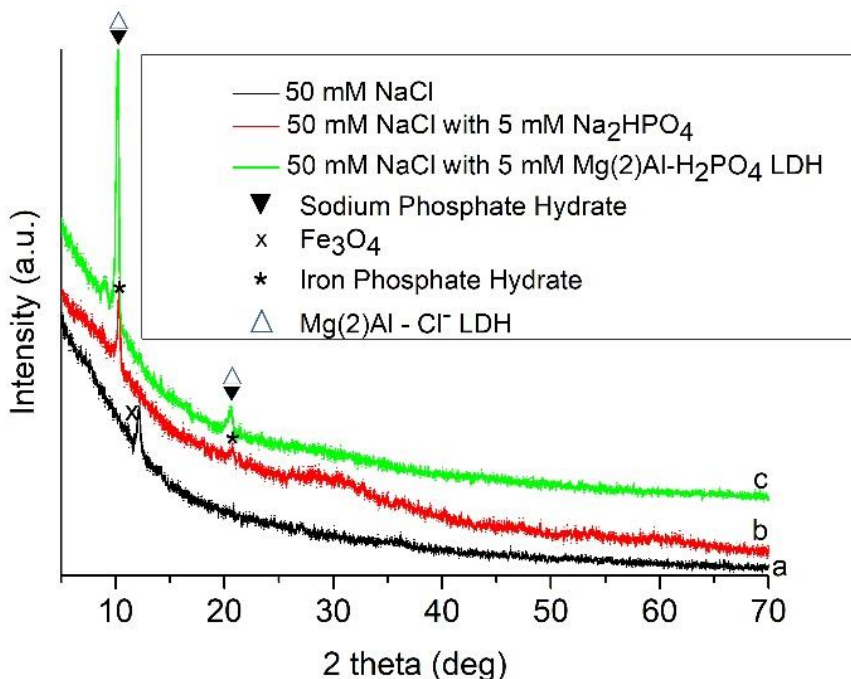


Fig. 29. XRD patterns of the corrosion products collected from the cast iron substrates immersed a) in a 50 mM NaCl solution, b) in a 50 mM NaCl + 5 mM Na<sub>2</sub>HPO<sub>4</sub> solution and c) in a 50 mM NaCl + 5 mM Mg(2)Al-H<sub>2</sub>PO<sub>4</sub> LDH solution.

It is seen from Fig. 29 that immersion in these three solutions resulted in precipitation and formation of different phases on the sample surface. The corrosion product formed in case of immersion in a 50 mM NaCl solution (the pattern *a*) is an iron oxide that is in good agreement with the optical photo (Fig. 26a). The XRD pattern *b* demonstrates a presence of iron phosphate hydrate. It is suggested that chlorine anions promote dissolution of iron from the substrate followed by reaction with Na<sub>2</sub>HPO<sub>4</sub> in the solution and a precipitation of iron phosphate. The corrosion products collected from the surface of the sample immersed in a 50 mM NaCl + 5 mM Mg(2)Al-H<sub>2</sub>PO<sub>4</sub> LDH solution (the pattern

c) seems to contain an LDH phase with the angle positions of the basal diffraction reflections that correspond to those of Mg(2)Al-Cl LDH. However, as its pattern overlaps that of sodium phosphate hydrate a distinction cannot be done. Also, peaks for iron phosphate hydrate can be found in the same sample.

In conclusion, the EIS results obtained for the samples immersed in the NaCl solution containing Mg(2)Al-10%Ce-H<sub>2</sub>PO<sub>4</sub> for 2-168 h were found to be essentially similar to those presented for the case of Mg(2)Al-H<sub>2</sub>PO<sub>4</sub> LDH. Ce<sup>III</sup>-containing species in the products of decomposition of the LDH nanocontainer itself may provide additional protection effect. However, to estimate such an effect, a much longer immersion time is needed alongside with the continuous exposition of the Mg(2)Al-10%Ce LDH to UV radiation to promote the LDH degradation. This study is in progress.

## 4. CONCLUSIONS

1. The Co/Mg/Al LDHs were successfully synthesized by the low supersaturation method, thermally decomposed and reconstructed in water or magnesium nitrate media. The partial substitution of the magnesium by cobalt showed changes in the LDHs behaviour during the cycle of synthesis – thermal decomposition – reconstruction. An incomplete regeneration of LDH samples at room temperature in aqueous media has been observed. However, with increasing temperature the reconstruction process of LDHs proceeded to completion.

2. It was demonstrated, that the reconstruction medium had a considerable influence on the morphology of mixed metal oxides. The  $N_2$  adsorption-desorption isotherms of heat-treated cobalt containing LDHs exhibited type IV isotherms with an H1 hysteresis which are characteristic for the mesoporous materials. The specific surface area of cobalt containing LDHs samples decreased upon reconstruction and calcination from  $170 \text{ m}^2 \text{ g}^{-1}$  for Co/Mg/Al<sub>cal</sub> to  $94 \text{ m}^2 \text{ g}^{-1}$  and  $131 \text{ m}^2 \text{ g}^{-1}$  for Co/Mg/Al<sub>W293</sub> and Co/Mg/Al<sub>W353</sub>, respectively. Moreover, a significant increase of specific surface area values were observed for the samples reconstructed in magnesium nitrate solution.

3. The bismuth containing LDH  $\text{Mg}_3\text{Al}_{1-x}\text{Bi}_x$  ( $x \leq 0.2$ ) were prepared by low saturation co-precipitation method from carbonate-containing solutions and for the first time to the best of our knowledge by an aqueous sol-gel processing. The XRD results showed that in the case of Mg/Al/Bi the both  $a$  and  $c$  parameters increased with increasing substitutional level of bismuth. Thus, the partial substitution of aluminium by bismuth occurred, since the ionic radius of  $\text{Bi}^{3+}$  is bigger than  $\text{Al}^{3+}$ . Sol-gel derived Mg/Al/Bi LDH consisted of the larger hexagonally shaped particles varying in size from approximately 200–500 nm. The good connectivity between the grains was also observed.

4. This study also investigated the temperature dependence of dielectric permittivity of  $\text{Mg}_3\text{Al}_{1-x}\text{Bi}_x$  LDH samples prepared by different methods. In general, the increase in  $\epsilon'$  was more pronounced at higher temperatures and at lower frequencies for non-vacuumed samples. The dielectric properties were independent on surface morphology of  $\text{Mg}_3\text{Al}_{1-x}\text{Bi}_x$  LDH samples fabricated by two different synthesis routes. Finally, no structural transitions were observed for all bismuth-doped LDH samples.

5. The influence of high power sonication on the intercalation of hydroxide, chloride and phosphate anions to the structure of the sol-gel derived magnesium-aluminium layered double hydroxides has been investigated. The XRD results demonstrated that sonication assisted reaction without mixing occurred much faster in comparison with reaction performed in water at 80 °C under the vigorous mechanical stirring. Monophasic  $\text{Mg}_2\text{Al}_1\text{-OH}_{(\text{Sonic}/\text{X})}$  LDH was obtained after 30 min of sonication. The intercalation reaction of  $\text{Cl}^-$  at room temperature proceeded 15 min, while sonication assisted anion exchange reaction completed during 4 min.

6. Sonication assisted method accelerated phosphate intercalation to the LDH reaction as well. The results of calculation of basal spacing showed a big increase of interlayer distance (from  $\sim 24 \text{ \AA}$  for  $\text{Mg}_2\text{Al}_1\text{-OH}$ ,  $\text{Mg}_2\text{Al}_1\text{-Cl}$  LDHs to  $\sim 30\text{-}32 \text{ \AA}$  for  $\text{Mg}_2\text{Al}_1\text{-PO}_4$  LDH). FT-IR, ICP-OES and TG results also confirmed the successful performance of intercalation reaction. SEM and STEM micrographs showed the formation of typical plate-like particles 0.5-2  $\mu\text{m}$  in size with hexagonal shape. In the case of  $\text{Mg}_2\text{Al}_1\text{-Cl}$  and  $\text{Mg}_2\text{Al}_1\text{-PO}_4$  LDHs the formation of plate-like hexagonal particles having lower crystallinity was determined.

7. The corrosion protection functionality of the Ce-substituted layered double hydroxide intercalated with dihydrogen phosphate ( $\text{Mg}_2\text{Al-10\%Ce-H}_2\text{PO}_4$ ) were studied as well. The efficiency of the layered double hydroxides produced using the novel approach as nanocontainers was demonstrated by electrochemical impedance spectroscopy results via corrosion protection effect of dihydrogen phosphate released from these LDH on cast iron substrate in a NaCl solution.



## 5. LIST OF PUBLICATIONS AND CONFERENCES PARTICIPATION

### 5.1. Articles in journals

1. D. Sokol, K. Klemkaite-Ramanauskė, A. Klynksis, K. Baltakys, A. Beganskiene, A. Baltusnikas, J. Pinkas, A. Kareiva. Reconstruction Effects on Surface Properties of Co/Mg/Al Layered Double Hydroxide, *Material Science*, Vol. 23, No.2. 2017. <http://dx.doi.org/10.5755/j01.ms.23.2.15184>
2. D. Sokol, A.N. Salak, M.G.S. Ferreira, A. Beganskiene, A. Kareiva. Bi-substituted Mg<sub>3</sub>Al–CO<sub>3</sub> layered double hydroxides, *Journal of Sol-Gel Science and Technology*. 85(1):1-10, 2017. DOI 10.1007/s10971-017-4506-9
3. D. Sokol, M. Ivanov, A.N. Salak, R. Grigalaitis, J. Banys, A. Kareiva. “Dielectric properties of Bi substituted LDHs synthesized by co-precipitation and sol-gel methods”. *Materials Science-Poland*. 37(2), 2019, pp. 190-195. DOI: 10.2478/msp-2019-0035
4. D. Sokol, D.E.L. Vieira, A. Zarkov, M.G.S. Ferreira, A. Beganskiene, V. V. Rubanik, A.D. Shilin, A. Kareiva & A.N. Salak. Sonication accelerated formation of Mg-Al-phosphate layered double hydroxide via sol-gel prepared mixed metal oxides. *Scientific reports*. Vol. 9 Article Nr. 10419, 2019. <https://doi.org/10.1038/s41598-019-46910>
5. D.E.L. Vieira, D. Sokol, A. Smalenskaite, A. Kareiva, M.G.S. Ferreira, J.M.Vieira, A.N. Salak. Cast iron corrosion protection with chemically modified Mg-Al layered double hydroxides synthesized using a novel approach. *Surface and Coatings Technology*. Vol. 375, p.p.158-163, 2019. <https://doi.org/10.1016/j.surfcoat.2019.07.028>

### 5.2. Attended conferences

1. D. Sokol, A.N. Salak, M.G. S. Ferreira, A. Kareiva, New double layered hydroxides: synthesis, properties and potential applications, *Abstracts of the International Conference “Functional Materials and Nanotechnologies” (FM&NT2017)*, Tartu, Estonia, P-53, 127 (2017).
2. D. Sokol, A. Beganskiene, A. Kareiva. New layered double hydroxides: synthesis, properties and possible application. *7-th Junior scientist conference. Interdisciplinary research in physical and technological science*. Vilnius, Lithuania (2017).

3. A. Kareiva, D. Sokol, M. Ivanov, A.N. Salak, R. Grigalaitis, M.G.S. Ferreira, A. Beganskiene, J. Banys, Bismuth substitution effects in Mg<sub>3</sub>/Al layered double hydroxides, *Abstracts of the International Conference on Oxide Materials for Electronic Engineering – fabrication, properties and applications (OMEE-2017)*, Lviv, Ukraine, Tu-P13, 251 (2017)
4. D. Sokol, A. Smalenskaite, A. Kareiva, V.V. Rubanik Jr., A.D. Shilin, V.V. Rubanik, D.E.L. Vieira, A.N. Salak, M.G.S. Ferreira, Ultrasound-assisted formation of multifunctional layered double hydroxides, *Proceedings of the II International conference on ultrasonic-based applications: from analysis to synthesis (ULTRASONICS-2016)* Caparica, Portugal, P11 (2016).
5. D. Sokol, A.N. Salak, M.G.S. Ferreira, A. Kareiva. Preparation of Ca/Al layered double hydroxide (LDH) with structural interlayer introduced metal oxide anions and their application as a catalyst in organic reactions. *6th International Conference on Materials and Applications for Sensors and Transducers*. Athens, Greece (2016)
6. D. Sokol, A.N. Salak, M.G.S. Ferreira, A. Kareiva, Bismuth substitution for magnesium and aluminium effects in Mg/Al/Bi layered double hydroxide, *Abstracts of the International Conference “NanoPortugal-2016” (nanoPT-2016)*, Braga, Portugal, P65 (2016).
7. D. Sokol, A. Kareiva. Synthesis of Mg/Al and Mg/Al/Bi layered double hydroxide via sol-gel and co-precipitation methods, decomposition and reconstruction. *International conference – school. Advanced materials and technologies*. 2016, Palanga, Lithuania.

## 6. ACKNOWLEDGEMENTS

First of all, I want to thank my supervisors Prof. Aivaras Kareiva and Prof. Jurgis Barkauskas for great knowledge, encouragement and support through all those study years. Thank you so much for trust and believe in me as a scientist and as a person. I am very grateful for having an opportunity to work, to communicate together and to get experience from such brilliant persons. Thank you for showing me directions and always being the best example.

I am also grateful to Dr. Kristina Klemkaite-Ramanauskė, my great scientific adviser, for huge help in all academic situations.

Moreover, I am truly thankful to Dr. Andrei Salak and Daniel Vieira from the Department of Materials and Ceramic Engineering, CICECO – Aveiro Institute of Materials for knowledge, for the help and successful collaboration during the PhD secondment at Aveiro University.

Furthermore, I sincerely thank all my colleges at the Department of Inorganic Chemistry for the help and assistance during the fulfillment of my scientific research, especially Dr. Aleksej Zarkov and Dr. Andrius Stanulis for the help, advices and tutorship in coping with difficulties that emerged during the process of scientific research and for their friendship.

Last, but not the least, I am deeply thankful to my amazing wife for giving me an opportunity to study, and for support during my ups and downs. Thank you for giving me wisdom, strength and faith.

## 7. REFERENCES

1. D. E. Evans, R. C. T. Slade, Structural aspects of layered double hydroxides. In *Structure and Bonding*; Springer-Verlag Berlin Heidelberg, 119 (2005) 1–87.
2. J. Twu, P. K. Dutta, *The Journal of Physical Chemistry*, 93, (1989) 7863-7868.
3. A. I. Khan, D. O'Hare, *RSC Journal of Material Chemistry*, 12, (2002) 3191-3198.
4. P. Vicente, M.E. Pérez-Bernal, R.J. Ruano-Casero, Duarte Ananias, F.A. Almeida Paz, J. Rocha, V. Rives, *Journal of Microporous and Mesoporous Materials*, 226, (2016) 209-220.
5. A. Smalenskaite, D.E.L. Vieira, A.N. Salak, M.G.S. Ferreira, A. Katelnikovas, A. Kareiva, *Applied Clay Science*. 143, (2017) 175-183.
6. A. Smalenskaite, S. Sen, A.N. Salak, M.G.S. Ferreira, A. Beganskiene and A. Kareiva, *Acta Physica Polonica A* 133, (2018) 884-886.
7. D. Sokol, A. N. Salak, M. G. S. Ferreira, A. Beganskiene, A. Kareiva, *Journal of Sol-Gel Science and Technology*, 85, (2017) 221-230.
8. A. Ennadi, A. Legrouri, A. De Roy, J. P Besse, *Journal of Solid-State Chemistry*, 152, (2000) 568-572.
9. E. Heraldry, S. J. Santosa, T. Tryono, K. Wijaya, *Indonesian Journal of Chemistry*, 15, (2015) 234-241.
10. J. He, M. Wei, B. Li, D. E. Evans, X. Duan, Structural aspects of layered double hydroxides. In *Structure and Bonding*; Springer-Verlag Berlin Heidelberg, 119 (2006) 89–119.
11. A. V. Radha, P. Vishnu Kamath, C. Shivakumara, *Journal of Physical Chemistry B*, 111, (2007) 3411-3418.
12. A. Ookubo, K. Ooi, H. Hayashi, *Langmuir*, 9, (1993) 1418-1422.
13. T. Tanaka, R. Tsukane, T. Matsuda, M. Imaoka, H. Tamai, *Resources Processing*, 63, (2016) 99-104.
14. S. B. Ghorbel, F. Medina, A. Ghorbel, A. M. Segarra, *Applied Catalysis A: General*, 493, (2015) 142-148.
15. F. Kovanda, E. Jindova, K. Lang, P. Kubat, Z. Sedlakova, *Applied Clay Science*, 48, (2010) 260-270.

16. G. Fan, F. Li, D. G. Evans, X. Duan, *RSC Chemical Society Review*, 43, (2014) 7040-7066.
17. V. Rives, M. Del Arco, C. Martín, *Journal of Controlled Release* 169, (2013) 28-39.
18. K. H. Goh, T. Lim, Z. Dong, *Water Resistant*, 42, (2008) 1343-1368.
19. M. Shao, F. Ning, J. Zhao, M. Wei, D. G. Evans, X. Duan, *Journal of American Chemical Society*, 134, (2012) 1071-1077.
20. X. Long, Z. Wang, S. Xiao, Y. An, S. Yang, *Materials Today*, 19, (2016) 213-226.
21. K. Yan, G. Wu, W. Jin, *Energy Technology*, 4, (2016) 354-368.
22. T. L.P. Galvao, C. S. Neves, A. P.F. Caetano, F. Maia, D. Mata, E. Malheiro, M. J. Ferreira, A. C. Bastos, A. N. Salak, J. R.B. Gomes, J. Tedim, M. G.S. Ferreira, *Journal of Colloid and Interface Science*, 468, (2016) 86–94.
23. D. Sokol, K. Klemkaite-Ramanauskė, A. Khinsky, K. Baltakys, A. Beganskiene, A. Baltusnikas, J. Pinkas, A. Kareiva, *Materials Science*, 23, (2017) 144-149.
24. P. Z. Xu, Q. G. Lu, *Chemistry of Materials*, 17, (2005) 1055-1062.
25. S. S. Shaflei, M. Soltai-Hashjin, H. Rahim-Zadeh, A. Samadikuchaksarei, *Advances in Applied Ceramic*, 112(1), (2013) 59-65.
26. A.S. Bookin, V.A. Drits, *Clays Clay Miner*, 41, 551.
27. A.S. Bookin, V.I. Cherkashin, V.A. Drits, *Clays Clay Miner*, 41, (1993) 558.
28. F. Cavani, F. Trifiro, A. Vaccari, *Catalysis Today*, 11, (1991) 173-301.
29. S. J. Mills, A. G. Christy, J.-M. R. Ge'nin, T. Kameda, F. Colombo, *Mineralogical Magazine*, 76(5), (2012) 1289–1336
30. F. Millange, R. I. Walton, D. O'Hare, *RSC Journal of Materials Chemistry*, 10, (2000) 1713-1720.
31. S. L. Wang, C. H. Lin, Y. Y. Yin, M. K. Wang, *Applied Clay Science*, 72 (2013) 191–195.
32. M. Meyn, K. Beneke, G. Lagaly, *Inorganic Chemistry*, 29, (1990) 5201-5207.
33. F. Millange, R.I. Walton, L. Lei, D. O'Hare, *Chemical Materials*, 12, (2000) 1990-1994.
34. F.M. Vichi, O.L. Alves, *Journal of Materials Chemistry*, 7, (1997) 1631-1634.

35. D. Srankó, A. Pallagi, E. Kuzmann, S.E. Canton, M. Walczak, A. Sápi, A. Kukovecz, Z. Kónya, P. Sipos, I. Pálinkó, *Applied Clay Science*, 48, (2010) 214-217.
36. C.G. Silva, Y. Bouizi, V. Fornés, H. García, *Journal of American Chemical Society*, 131, (2009) 13833–13839.
37. F. Geng, Y. Matsushita, R. Ma, H. Xin, M. Tanaka, F. Izumi, N. Iyi, T. Sasaki, *Journal of American Chemical Society*, 130 (2008) 16344–16350.
38. A. Smalenskaite. Layered double hydroxides: synthesis, characterization, modification and lanthanide ions substitution effects on luminescent properties. Vilnius University, Vilnius, Lithuania, 2020, 156 p.
39. L. A. Utracki, M. Sepehr, E. Boccaleri, *Polymers for Advanced Technologies*, 18 (2007) 1-37.
40. M. R. Othman, Z. Helwani, Martunus, W. J. N. Fernando. *Applied Organometallic Chemistry*, 23 (2009) 335-346.
41. L. Valeikiene, R. Paitian, I. Grigoraviciute-Puroniene, K. Ishikawa, *Materials Chemistry and Physics*, **237** (2019) 121863.
42. K. Binnemans, *Chemical Reviews*, 109 (2009) 4283-4374.
43. K. Klemkaite, I. Prosycevas, R. Taraskevicius, A. Khinsky, A. Kareiva, *Central European Journal of Chemistry*, 9 (2011) 275-282.
44. H.W. Olf, L.O. Torres-Dorante, R. Eckelt, H. Kosslick, *Applied Clay Science*, 43 (2009), 459-464.
45. K. Parida, M. Satpathy, L. Mohapatra, *Journal of Materials Chemistry*, 22 (2012) 7350–7357.
46. K. Klemkaite-Ramanauske. Synthesis, modification and characterization of Mg/Al, Co/Mg/Al and Ni/Mg/Al layered double hydroxides. Vilnius University, Vilnius, Lithuania, 2012, 89 p.
47. X. Wang, X. Zhu, X. Meng, *RSC Advance*, 7 (2017) 34984-34993.
48. M. Laipan, H. Fu, R. Zhu, L. Sun, J. Zhu, H. He, *Scientific Reports*, 7: 7277 (2017) 1-11.
49. L. Alidokht, S. Oustan, A. Khataee, M. Neyshabouri, A. Reyhanitabar, *Research on Chemical Intermediates*, 44 (2018) 2319-2331.
50. S. Chen, Y. Huang, X. Han, Z. Wu, C. Lai, J. Wang, Q. Deng, Z. Zeng, S. Deng, *Chemistry Engineering Journal*, 352 (2018), 306-315.
51. A.N. Salak, A.D. Lisenkov, M.L. Zheludkevich, M.G.S. Ferreira, *ECS Electrochemistry Lett.* 3 (2014) C9–C11.

52. M. Serdechnova, A.N. Salak, F.S. Barbosa, D.E.L. Vieira, J. Tedim, M.L. Zheludkevich, M.G.S. Ferreira, *Journal of Solid State Chemistry*, 233 (2016) 158–165.
53. H.J. Li, X.Y. Su, C.H. Bai, Y.Q. Xu, Z.C. Pei, S.G. Sun, *Sensors and Actuators. B- Chemical*, 225, (2016) 109–114.
54. P. Lu, S. Liang, L. Qiu, Y.S. Gao, Q. Wang, *Journal of Membrane Science*, 504 (2016) 196–205.
55. V. R. Rodrigues Cunha, R. Barbosa de Souza, A. M. C. Rebello Pinto da Fonseca Martins, I. Hong Jun Koh, V. R. Leopoldo Constantino, *Scientist Reports*, 6 (2016) Art. No. 30547.
56. M.A. Djebbi, Z. Bouaziz, A. Elabed, M. Sadiki, S. Elabed, *International Journal of Pharmaceutics*, 506 (2016) 438-448.
57. G. Carja, E.F. Grosu, C. Petrarean, N. Nichita, *Nano Research*, 11 (2015) 3512-3523.
58. C.T. Gore, S. Omwoma, W. Chen, *Chemical Engineering Journal*, 284 (2016) 794–801.
59. E. F. Grosu, D. Simiuc, R. Froidevaux, *Biomedical Journal Scientific and Technical Research*, 2 (2018) 2747-2752.
60. Z. Cao, N. N. M. Adnan, G. Wang, A. Rawal, B. Shi, R. Liu, K. Liang, L. Zhao, J. J. Gooding, C. Boyer, Z. Gu, *Journal of Colloid and Interference Science*, 521 (2018) 242-251.
61. A. C. Luca, L. D. Duceac, G. Mitrea, M. I. Ciuhodaru, D. L. Ichim, G. Baciuc, E. A. Banu, A. C. Iordache, *Materiale Plastice*, 55 (2018) 552-554.
62. M.F. Montemor, D.V. Snihirova, M.G. Taryba, S.V. Lamaka, I.A. Kartsonakis, A.C. Balaskas, *Electrochimica Acta*, 60 (2012), 31-40.
63. M.L. Zheludkevich, S.K. Poznyak, L.M. Rodrigues, D. Raps, T. Hack, L.F. Dick, *Corrosion Science*, 52 (2) (2010) 602-611.
64. M.L. Zheludkevich, J. Tedim, C.S.R. Freire, S.C.M. Fernandes, S. Kallip, A. Lisenkov, *Journal of Materials Chemistry*, 21 (2011) 4805-4812.
65. L. Perioli, P. Mutascio, C. Pagano, *Pharmaceutical Research*, 30 (2013) 156-166.
66. L. Guo, F. Zhang, J.C. Lu, R.C. Zeng, S.Q. Li, L. Song, J.M. Zeng, *Frontiers of Materials Science*, 12(2) (2018) 198–206.
67. X. Hu, X. Gao, *Physical Chemistry Chemical Physics*, 13 (2011) 10028–10035.

68. Y. Zhao, J.G. Li, F. Fang, N. Chu, H. Ma, X. Yang, Dalton Transactions, 41 (2012) 12175–1218.
69. Y. Sohn, Ceramics International, 40 (2014) 13803-13811.
70. S. Li, H. Qin, R. Zuo, Z. Bai, Applied Surface Science, 353 (2015) 643–650.
71. H.N. Tran, C. Lin, S.H. Woo, H.P. Chao, Applied Clay Science, 154 (2018) 17–27.
72. A. Smalenskaite, S. Şen, A.N. Salak, M.G.S. Ferreira, R. Skaudzius, A. Katelnikovas, A. Kareiva, Current Inorganic Chemistry, 6 (2016) 149-154.
73. A. Smalenskaite, L. Pavasaryte, Thomas C.K. Yang, A. Kareiva, Materials, 12, 736 (2019) 1-14.
74. A. Smalenskaite, A.N. Salak, M.G.S. Ferreira, R. Skaudzius, A. Kareiva, Optical Materials, 80 (2018) 186–196.
75. A. Smalenskaite, A.N. Salak, A. Kareiva, Mendeleev Communications, 28 (2018) 493-494.
76. S. Ribet, D. Tichit, B. Coq, B. Ducourant, F. Morato, Journal of Solid State Chemistry, 142, (1999) 382-392.
77. J.Perez-Ramirez, S. Abello, N.M.Van Der Pers, The Journal of Physical Chemistry C, 111, (2007) 3642-3650.
78. D.E. Sparks, T. Morgan, P.M. Patterson, S.A. Tackett, E. Morris, M. Crocker, Applied Catalysis B-Environmental, 82 (2008) 190-198.
79. M. Ivanov, K. Klemkaite, A. Khinsky, A. Kareiva, J. Banys, Ferroelectrics, 417 (2011) 136-142.
80. P. Kaur, S. Bahel, S.B. Narang, Materials Research Bulletin, 100 (2018) 275-281.
81. S. Duhan, S. Sanghi, A. Agarwal, A. Sheoran, S. Rani, Physica B: Condensed Matter, 404 (2009) 1648–1654.
82. J. Pozingis, J. Macutkevicius, R. Grigalaitis, J. Banys, D.C. Lupascu, Ceramics International, 40 (2014) 9961–9969.
83. M.M. Vijatovic Petrovic, R. Grigalaitis, N. Ilic, J.D. Bobic, A. Dzunuzovic, J. Banys, B.D. Stojanovic, Journal of Alloys and Compounds, 724 (2017) 959-968.
84. S. Luo, K. Wang, Scripta Materialia, 146 (2018) 160-163.
85. M.N. Siddique, A. Ahmed, P. Tripathi, Journal of Alloys and Compounds, 735 (2018) 516-529.



86. G. W. Brindley, C. C. Kao, *Physics and Chemistry of Minerals*, 10 (1984) 187-191.
87. A. N. Salak, J. Tedim, A. I. Kuznetsova, L. G. Vieira, J. L. Ribeiro, M. L. Zheludkevich, M. G. S. Ferreira, *The Journal of Physical Chemistry C*, 117, 4152-4157 (2013).
88. D. Sokol, D.E.L. Vieira, A. Zarkov, M.G.S. Ferreira, A. Beganskiene, V.V. Rubanik, A.D. Shilin, A. Kareiva, A.N. Salak, *Scientific reports*, 9 (2019) 10419.
89. I.G. Richardson, *Acta Crystallographica Section B: Structural Science, Crystal Engineering and Materials*, 69 (2013) 150–162.

## 8. SUMMARY IN LITHUANIAN

## ĮVADAS

Sluoksniuoti dvigubi hidroksidai (SDH), taip pat žinomi kaip hidrotalcito tipo (HT) junginiai, priklauso anijoninių molžemių šeimai, kurių kristalinė struktūra sudaryta iš brusito,  $Mg(OH)_2$ . SDH teigiamą krūvį turintis mišrių metalų katijonų hidroksidų sluoksnis yra kompensuojamas tarp sluoksnyje esančiais anijonais  $A^{m-}$ , kordinuotais vandens molekulėmis. Nors yra žinomi  $M^I$ - $M^{III}$  SHD, tačiau dauguma sluoksniuotų dvigubų hidroksidų yra  $M^{II}$ - $M^{III}$  tipo. Bendrinė SDH cheminė formulė gali būti išreikšta taip:  $[M^{II}_x \cdot M^{III}_y(OH)_2]^{x+}(A^{m-})_{x/m} \cdot zH_2O$ . Dažniausiai  $M^{II}$  katijonas yra magnis (Mg) arba kiti 4-ojo periodo pereinamieji metalai, nuo geležies iki cinko, o  $M^{III}$  katijonai, kaip taisyklė, yra Al, Ga, Fe arba Cr. Naujausi darbai parodė jog  $M^{III}$  katijonai, esantys SHD, gali būti iki 10mol% pakeisti didelio joninio spindulio lantanoidais. Dažniausiai naudojamuose sluoksniuotuose dvigubuose hidroksiduose katijonų  $M^{II}/M^{III}$  santykis yra tarp 2 ir 3, nors jis gali kisti ir nuo 1 iki maždaug 5. Skirtingi sluoksnių krūvių santykiai, sukurti dėl katijonų  $M^{II}/M^{III}$  santykio ir kristalinės struktūros labilumo, leidžia formuoti didelį kiekį SDH su tarp sluoksnyje esančia didele organinių ir neorganinių anijonų įvairove.

Sluoksniuoti dvigubi hidroksidai plačiai taikomi įvairiose srityse, tokiose kaip korozijos inhibitoriai, katalizatoriai, vaistinių medžiagų nešikliai, adsorbentai, energijos saugojimo ir išskyrimo medžiagos. Dauguma SHD gaminamų pramoniniu būdu yra sintetiniai bendro nusodinimo, hidroterminiu arba kombinuotu (bendras nusodinimas ir hidroterminis) sintezės metodais. Šie sintezės metodai leidžia nuolat paruošti aukšto kristališkumo medžiagas, tačiau tokios sintezės trunka labai ilgai bei reikalauja didelio kiekio vandens. Todėl naujų SDH sintezės metodų paieška šiuo metu yra itin svarbus uždavinys medžagotyriminkams.

Šiame moksliniame darbe pateikiami tobulesnio SHD junginių sintezės metodo išvystymo rezultatai ir atskleistos naujos susintetintų junginių fizikinės ir mikrostruktūrinės savybės. Naujų SDH cheminių sudėčių paieška, keičiant magnį ir aliuminį kitais katijonais ir/arba įvedant skirtingus anijonus, yra nemažas indėlis į šių medžiagų mokslo teorinius pagrindus. Minėti mokslinių tyrimų ir gautų rezultatų ypatumai ir yra šios daktaro disertacijos **naujumas ir originalumas**.

**Šios daktaro disertacijos tikslas** buvo ištirti, kaip katijonų ir anijonų pakeitimas Mg-Al sluoksniuotose dvigubuose hidroksiduose veikia junginių

formavimąsi ir savybes. Šiam tikslui įgyvendinti buvo suformuluoti šie disertacijos uždaviniai:

1. Ištirti magnio pakeitimo kobaltu Co-Mg-Al sluoksniuotame dvigubame hidrokside, kuris buvo susintetintas naudojant mažų koncentracijų bendro nusodinimo metodą, galimybes bei susintetintų ir rekonstruotų SHD skirtingose rekonstrukcinėse terpėse paviršiaus savybes.
2. Pirmą kartą susintetinti bismutu ( $\text{Bi}^{3+}$ ) pakeistą Mg-Al SDH tiesioginiu bendro nusodinimo ir nauju netiesioginiu vandeniniu zolių-gelių metodais ir ištirti įvairių parametru įtaką Bi-Mg-Al sluoksniuotų dvigubų hidroksidų susidarymui.
3. Ištirti Bi-Mg-Al SHD, susintetintų bendro nusodinimo ir vandeniniu zolių-gelių metodais, dielektrines savybes.
4. Ištirti ultragarso poveikį Mg-Al SDH, sintetinto zolių-gelių metodu, rekonstravimo ir anijonų pakeitimo galimybėms.
5. Ištirti chemiškai modifikuotų Mg-Al SDH junginių antikorozinės savybes.

Gauti eksperimentinių tyrimų rezultatai yra aptarti disertacijos Rezultatų ir jų aptarimų dalyje. Disertacijos 3.1. dalyje ištirtos magnio pakeitimo kobaltu Co-Mg-Al sluoksniuotame dvigubame hidrokside, kuris buvo susintetintas naudojant mažų koncentracijų bendro nusodinimo metodą, galimybės bei susintetintų ir rekonstruotų Co/Mg/Al SHD skirtingose rekonstrukcinėse terpėse paviršiaus savybės. Šio disertacinio darbo 3.2. ir 3.3 dalyse pateikti bismutu ( $\text{Bi}^{3+}$ ) pakeistų Mg-Al SDH junginių, susintetintų tiesioginiu bendro nusodinimo ir nauju netiesioginiu vandeniniu zolių-gelių metodais, tyrimų rezultatai. Disertacijos 3.4. dalyje ištirtas ultragarso poveikis Mg-Al SDH, sintetinto zolių-gelių metodu, rekonstravimo ir anijonų pakeitimo galimybėms, o 3.5. dalyje buvo ištirtos chemiškai modifikuotų Mg-Al SDH junginių antikorozinės savybės. Visi daktaro disertacijos rezultatai yra apibendrinti 5-iuose moksliniuose straipsniuose, kurie pateikti disertacijos pabaigoje. Gauti duomenys yra apibendrinti išvadose.

## IŠVADOS

1. Co/Mg/Al sluoksniuoti dvigubi hidroksidai buvo sėkmingai susintetinti žemos koncentracijos bendro nusodinimo metodu, termiškai suskaidyti ir rekonstruoti vandenyje arba magnio nitrato

- terpėje. Dalinis magnio pakeitimas kobaltu įtakojo SHD sintezės – terminio skaidymo – rekonstravimo ciklą. Kambario temperatūroje naudojant vandeninę terpę patebėtas nepilnas sluoksniuotų dvigubų hidroksidų rekonstravimas, tačiau pakėlus rekonstravimo temperatūrą, SHD rekonstravimo procesas buvo užbaigtas sėkmingai.
2. Įrodyta, jog rekonstrukcijos terpė daro didelę įtaką mišrių metalų oksidų (MMO) morfologijai. Nustatyta, kad termiškai apdoroto SDH, turinčio kobalto,  $N_2$  adsorbcijos-desorbcijos izotermos buvo IV tipo su H1 histereze, kuri yra būdinga mezoporinėms medžiagoms. Kobaltą turinčių SDH mėginių specifinis paviršiaus plotas juos rekonstruojant ir termiškai skaidant atitinkamai sumažėjo nuo  $170 \text{ m}^2 \text{ g}^{-1} \text{ Co/Mg/Al}_{\text{cal}}$  iki  $94 \text{ m}^2 \text{ g}^{-1}$  ir  $131 \text{ m}^2 \text{ g}^{-1} \text{ Co/Mg/Al}_{\text{W293}}$  ir  $\text{Co/Mg/Al}_{\text{W353}}$ . Taip pat nustatyta, kad mėginių, rekonstruotų magnio nitrato tirpale, specifinio paviršiaus ploto vertės padidėjo.
  3. Bismutą turintys  $\text{Mg}_3\text{Al}_{1-x}\text{Bi}_x$  ( $x \leq 0.2$ ) SDH buvo susintetinti mažų koncentracijų bendro nusodinimo metodu iš karbonatus turinčių tirpalų ir pirmą kartą vandeniniu zolių-gelių metodu. Rentgeno spindulių difrakcijos rezultatai parodė, jog  $\text{Mg/Al/Bi}$  SDH abu  $a$  ir  $c$  parametrai padidėjo didinant įvedamo bismuto kiekį. Tai rodo, jog įvyko dalinis aliuminio pakeitimas bismutu, nes  $\text{Bi}^{3+}$  joninis spindulys yra didesnis nei  $\text{Al}^{3+}$ . Zolių-gelių gauti  $\text{Mg/Al/Bi}$  SDH buvo sudaryti iš didesnių šešiakampių formos dalelių, kurių dydis svyravo nuo maždaug 200 iki 500 nm.
  4. Šiame darbe taip pat ištirta skirtingais sintezės metodais susintetintų  $\text{Mg}_3\text{Al}_{1-x}\text{Bi}_x$  SDH mėginių dielektrinio laidumo priklausomybė nuo temperatūros. Iš esmės  $\epsilon'$  padidėjimas nevakuuotuose mėginiuose buvo ryškensis esant aukštesnei temperatūrai ir žemesniam dažniui. Dielektrinės savybės nepriklausė nuo  $\text{Mg}_3\text{Al}_{1-x}\text{Bi}_x$  SDH mėginių, pagamintų dviem skirtingais sintezės būdais, paviršiaus morfologijos. Įdomu pažymėti, kad bismutu legiruotuose SDH mėginiuose nebuvo pastebėta jokių struktūrinių virsmų.
  5. Ištirta didelės galios ultragarso įtaka hidroksidų, chloridų ir fostatų anijonų interkaliacijai (įterpimui į tarpsluosnį) zolių-gelių metodu susintetintuose magnio-aliuminio sluoksniuotuose dvigubuose hidrosiduose ir gautų interkaliatų struktūrai. Rentgeno spindulių difrakcijos duomenys parodė, jog ultragarsu vykdoma reakcija be mechaninio maišymo vyko daug greičiau nei reakcija kuri buvo vykdoma  $80 \text{ }^\circ\text{C}$  vandenyje, intensyviai mechaniškai maišant. Ultragarsu vykdytos reakcijos metu vienfazis  $\text{Mg}_2\text{Al}_1\text{-OH}_{(\text{Sonic}/X)}$  SDH

buvo gautas jau po 30 min. Chlorido anijono interkaliacija kambario temperatūroje vyko 15 min., o ultragarsu vykdytas anijono visiškasis pakeitimas įvyko per 4 min.

6. Naudotas ultragarso metodas taip pat pagreitino ir fostatų įterpimą į SDH tarpsluoksnį. Bazalinio sluoksnio skaičiavimo rezultatai parodė tarpsluoksnio atstumo padidėjimą (nuo ~24 Å  $Mg_2Al_1-OH$  ir  $Mg_2Al_1-Cl$  SDH iki ~30-32 Å  $Mg_2Al_1-PO_4$  SDH). FT-IR, ISP-OES ir TG rezultatai tai pat patvirtino sėkmingą įterpimo reakcijos atlikimą. SEM ir SPEM tyrimais gauti duomenys atskleidė būdingų šešiakampės formos plokščių dalelių, kurių dydis 0.5-2 μm, susidarymą.  $Mg_2Al_1-Cl$  ir  $Mg_2Al_1-PO_4$  SDH atveju buvo nustatytas mažesnis šešiakampės formos plokščių dalelių kristališkumas.
7. Taip pat ištirtas ceriu ( $Ce^{3+}$ ) legiruoto sluoksnuoto dvigubo hidroksido su tarpsluoksnyje įterptu dihidrofosfatu ( $Mg_2Al_1-10\%Ce-H_2PO_4$ ) apsaugos nuo korozijos funkcionalumas. Sluoksnuotų dvigubų hidroksidų, gautų taikant naują sintezės metodą, o tiksliau - naudojant juos kaip nanokonteinerius, efektyvumas buvo įrodytas elektrocheminės varžos spektroskopijos rezultatais, panaudojus dihidrofosfato, išsiskiriančio iš šių SDH, apsaugos nuo korozijos efektą ketaus padėklui NaCl tirpale.

## GYVENIMO APRAŠYMAS CURRICULUM VITAE

1. Vardas: Denis
2. Pavardė: Sokol
3. Gimimo data: 1986-10-10
4. Pilietybė: Lietuvos Respublikos
5. Adresas namų: Genių g. 4-48, LT-11208 Vilnius
6. Telefonas: +37060046968
7. El. paštas: [denis.sokol.chf@gmail.com](mailto:denis.sokol.chf@gmail.com)
8. Išsilavinimas

<b>Institucija:</b>	<b>Baigimo metai</b>	<b>Specialybė</b>
Vilniaus Universitetas	2009	Chemiko bakalauro laipsnis
Vilniaus Universitetas	2011	Chemiko magistro laipsnis
Vilniaus Universitet	2014-2018	Studijos doktorantūroje

9. Darbo patirtis

<b>Data (nuo-iki)</b>	<b>Institucija</b>	<b>Pareigos</b>
2007-02-07 – 2009-03-01	Vilniaus universiteto Taikomųjų mokslų instituto Skystųjų kristalų laboratorija	Technikas
2009-03-01 – 2011-08-19	UAB „Tiksloji sintezė“	Inžinierius tyrėjas
2011-08-22 – 2013-08-09	UAB „Sicor Biotech“	Veikliosios vaistinės medžiagos gamybos skyriaus technologas
2013-08-12 – 2014-09-08	UAB „Interautomatika“	Produktų grupės vadovas
2014-12-10 – 2017-08-31	Vilniaus Universitetas, Chemijos fakultetas	Vyresnysis specialistas

2017-08-31 – 2018-01-31	Vilniaus Universitetas, Chemijos ir Geomokslų fakultetas, Chemijos institutas	Profesoriaus asistentas
2017-08-31 – 2018-08-03	UAB “Gym plius”	Eksploatacijos Vadovas
2018-09-10 – 2019-05-01	UAB “Project group”	Statybų ir Eksploatacijos vadovas

10. Kita patirtis (*Dalyvavimas organizacijose, komitetuose, ekspertinė veikla, apdovanojimai*)

<b>Data</b>	<b>Programa, projektai</b>
<b>2015-2018</b>	ES programa HORIZON 2020 MSCA-RISE-2014: Marie Skłodowska-Curie Research and Innovation StaffExchange (RISE) project „TUMOCS: TUneable Multiferroics based on oxygen Octahedral Structures”, Aveiro, Portugalija.

11. Kita svarbi informacija (*Atskleidžianti turimas kompetencijas, kvalifikacijos kėlimas*).

<b>Data</b>	<b>Įstaiga</b>
<b><i>Kvalifikacijos kėlimas (mokslinės stažuotės):</i></b>	
2016 m. (1 mėn.)	Mokslinė stažuotė Aveiro universitete, Portugalija, TUMOCS projekto kvietimu.
2016 m. (1 mėn.)	Mokslinė stažuotė Minskas, (Scientific-practical materials research center of national academy of science of Belarus, Baltarusija, TUMOCS projekto kvietimu.
2017 m. (1 mėn.)	Mokslinė stažuotė Aveiro universitete, Portugalija, TUMOCS projekto kvietimu.



2014-2015 m.	Vadovas, Neorganinės katedros bakalauro studijų studento.
2015-2016 m.	Vadovas, Neorganinės katedros bakalauro studijų studentės.
2016-2017 m.	Vadovas, Neorganinės katedros bakalauro studijų studento.
2016 m. (3d.)	International workshop on Metastable Perovskite Multiferroics, (Institute of Technical Acoustics of Scientific Practical Materials Research Centre of National Academy of Science of Belarus).

# MOKSLINIŲ PUBLIKACIJŲ DISERTACIJOS TEMA SĄRAŠAS IR JŲ KOPIJOS

Straipsniai recenzuojamuose žurnaluose:

1. D. Sokol, K. Klemkaite-Ramanauskė, A. Klynksi, K. Baltakys, A. Beganskiene, A. Baltusnikas, J. Pinkas, A. Kareiva. Reconstruction Effects on Surface Properties of Co/Mg/Al Layered Double Hydroxide, *Material Science*, Vol. 23, No.2. 2017. <http://dx.doi.org/10.5755/j01.ms.23.2.15184>
2. D. Sokol, A.N. Salak, M.G.S. Ferreira, A. Beganskiene, A. Kareiva. Bi-substituted Mg<sub>3</sub>Al–CO<sub>3</sub> layered double hydroxides, *Journal of Sol-Gel Science and Technology*. 85(1):1-10, 2017. DOI 10.1007/s10971-017-4506-9
3. D. Sokol, M. Ivanov, A.N. Salak, R. Grigalaitis, J. Banys, A. Kareiva. “Dielectric properties of Bi substituted LDHs synthesized by co-precipitation and sol-gel methods”. *Materials Science-Poland*. 37(2), 2019, pp. 190-195. DOI: 10.2478/msp-2019-0035
4. D. Sokol, D.E.L. Vieira, A. Zarkov, M.G.S. Ferreira, A. Beganskiene, V. V. Rubanik, A.D. Shilin, A. Kareiva & A.N. Salak. Sonication accelerated formation of Mg-Al-phosphate layered double hydroxide via sol-gel prepared mixed metal oxides. *Scientific reports*. Vol. 9 Article Nr. 10419, 2019. <https://doi.org/10.1038/s41598-019-46910>
5. D.E.L. Vieira, D. Sokol, A. Smalenskaite, A. Kareiva, M.G.S. Ferreira, J.M.Vieira, A.N. Salak. Cast iron corrosion protection with chemically modified Mg-Al layered double hydroxides synthesized using a novel approach. *Surface and Coatings Technology*. Vol. 375, p.p.158-163, 2019. <https://doi.org/10.1016/j.surfcoat.2019.07.028>

Pranešimų mokslinėse konferencijose tezės:

1. D. Sokol, A.N. Salak, M.G. S. Ferreira, A. Kareiva, New double layered hydroxides: synthesis, properties and potential applications, *Abstracts of the International Conference “Functional Materials and Nanotechnologies” (FM&NT2017)*, Tartu, Estonia, P-53, 127 (2017).
2. D. Sokol, A. Beganskiene, A. Kareiva. New layered double hydroxides: synthesis, properties and possible application. *7-th Junior scientist conference. Interdisciplinary research in physical and technological science*. Vilnius, Lithuania (2017).

3. A. Kareiva, D. Sokol, M. Ivanov, A.N. Salak, R. Grigalaitis, M.G.S. Ferreira, A. Beganskiene, J. Banys, Bismuth substitution effects in Mg<sub>3</sub>/Al<sub>1</sub> layered double hydroxides, *Abstracts of the International Conference on Oxide Materials for Electronic Engineering – fabrication, properties and applications (OMEE-2017)*, Lviv, Ukraine, Tu-P13, 251 (2017)
4. D. Sokol, A. Smalenskaite, A. Kareiva, V.V. Rubanik Jr., A.D. Shilin, V.V. Rubanik, D.E.L. Vieira, A.N. Salak, M.G.S. Ferreira, Ultrasound-assisted formation of multifunctional layered double hydroxides, *Proceedings of the II International conference on ultrasonic-based applications: from analysis to synthesis (ULTRASONICS-2016)* Caparica, Portugal, P11 (2016).
5. D. Sokol, A.N. Salak, M.G.S. Ferreira, A. Kareiva. Preparation of Ca/Al layered double hydroxide (LDH) with structural interlayer introduced metal oxide anions and their application as a catalyst in organic reactions. *6th International Conference on Materials and Applications for Sensors and Transducers*. Athens, Greece (2016)
6. D. Sokol, A.N. Salak, M.G.S. Ferreira, A. Kareiva, Bismuth substitution for magnesium and aluminium effects in Mg/Al/Bi layered double hydroxide, *Abstracts of the International Conference “NanoPortugal-2016” (nanoPT-2016)*, Braga, Portugal, P65 (2016).
7. D. Sokol, A. Kareiva. Synthesis of Mg/Al and Mg/Al/Bi layered double hydroxide via sol-gel and co-precipitation methods, decomposition and reconstruction. *International conference – school. Advanced materials and technologies*. 2016, Palanga, Lithuania.